Monthly Notices
of the
ROYAL ASTRONOMICAL SOCIETY

Mon. Not. R. Astron. Soc. **424,** 649–665 (2012) doi:10.1111/j.1365-2966.2012.21244.x

# The complex case of V445 Lyr observed with *Kepler*: two Blazhko modulations, a non-radial mode, possible triple mode RR Lyrae pulsation, and more

E. Guggenberger,[1⋆] K. Kolenberg,[2,3] J. M. Nemec,[4] R. Smolec,[1,5] J. M. Benkő,[6] C.-C. Ngeow,[7] J. G. Cohen,[8] B. Sesar,[8] R. Szabó,[6] M. Catelan,[9] P. Moskalik,[5] K. Kinemuchi,[10] S. E. Seader,[11] J. C. Smith,[11] P. Tenenbaum[11] and H. Kjeldsen[12]

[1]*Institut für Astronomie, Universität Wien, Türkenschanzstrasse 17, A-1180 Vienna, Austria*
[2]*Harvard–Smithsonian Center for Astrophysics, 60 Garden Street, Cambridge, MA 02138, USA*
[3]*Instituut voor Sterrenkunde, Celestijnenlaan 200D, B-3001 Leuven, Belgium*
[4]*Department of Physics & Astronomy, Camosun College, Victoria, British Columbia V8P 5J2, Canada*
[5]*Copernicus Astronomical Center, Polish Academy of Sciences, ul. Bartycka 18, 00-716 Warszawa, Poland*
[6]*Konkoly Observatory, Research Center for Astronomy and Earth Sciences, PO Box 67, H-1525 Budapest, Hungary*
[7]*Graduate Institute of Astronomy, National Central University, Jhongli City, Taoyuan County 32001, Taiwan*
[8]*California Institute of Technology, Mail Stop 249-17, 1200 East California Boulevard, Pasadena, CA 91125, USA*
[9]*Departamento de Astronomía y Astrofísica, Facultad de Física, Pontificia Universidad Católica de Chile, Av. Vicuña Mackenna 4860, 782-0436 Macul, Santiago, Chile*
[10]*NASA Ames Research Center/Bay Area Environmental Research Institute, Mail Stop 244-30, Moffett Field, CA 94035, USA*
[11]*SETI Institute/NASA Ames Research Center, Moffett Field, CA 94035, USA*
[12]*Department of Physics and Astronomy, Aarhus University, DK-8000 Aarhus C, Denmark*

Accepted 2012 May 4. Received 2012 April 30; in original form 2012 February 23

## ABSTRACT

Rapid and strong changes in the Blazhko modulation of RR Lyrae stars, as have recently been detected in high-precision satellite data, have become a crucial topic in finding an explanation of the long-standing mystery of the Blazhko effect. We present here an analysis of the most extreme case detected so far, the RRab star V445 Lyr (KIC 6186029) which was observed with the *Kepler* space mission. V445 Lyr shows very strong cycle-to-cycle changes in its Blazhko modulation, which are caused by both a secondary long-term modulation period and irregular variations. In addition to the complex Blazhko modulation, V445 Lyr also shows a rich spectrum of additional peaks in the frequency range between the fundamental pulsation and the first harmonic. Among those peaks, the second radial overtone could be identified, which, combined with a metallicity estimate of [Fe/H] = −2.0 dex from spectroscopy, allowed us to constrain the mass (0.55–0.65 $M_{\odot}$) and luminosity (40–50 $L_{\odot}$) of V445 Lyr through theoretical Petersen diagrams. A non-radial mode and possibly the first overtone are also excited. Furthermore, V445 Lyr shows signs of the period-doubling phenomenon and a long-term period change. A detailed Fourier analysis along with a study of the O − C variation of V445 Lyr is presented, and the origin of the additional peaks and possible causes of the changes in the Blazhko modulation are discussed. The results are then put into context with those of the only other star with a variable Blazhko effect for which a long enough set of high-precision continuous satellite data has been published so far, the *CoRoT* star 105288363.

**Key words:** asteroseismology – methods: data analysis – techniques: photometric – stars: individual: KIC 6186029 (V445 Lyr) – stars: individual: CoRoT 105288363 – stars: variables: RR Lyrae.

## 1 INTRODUCTION

RR Lyrae stars, which are low-mass helium-burning stars on the horizontal branch, were long thought to be rather simple radial pulsators. They follow a period–luminosity–colour relation which makes them valuable distance indicators, and because of their age

⋆E-mail: elisabeth.guggenberger@univie.ac.at

and evolutionary status, they are also used to study the formation and evolution of the Galaxy (Catelan 2009). They can oscillate in the fundamental radial mode (type RRab), the first overtone (type RRc) or both modes simultaneously (type RRd), and their high amplitudes of up to 1.5 mag in $V$ for RRab type stars made their variability easy to discover, so they have been known since the end of the 19th century.

Already more than a hundred years ago, however, it turned out that there is an aspect to RR Lyrae stars which is not understood at all: Blazhko (1907) found a 'periodic change in the period' of RW Dra, which he could not explain, and which still remains unexplained today. Shapley (1916) later found in his observations of RR Lyrae that the brightness of the maxima and the light-curve shape also show periodic changes. With increasing data quality in the recent past, the unsolved problem got even more severe, as it turned out that not just a rather small fraction of exceptional RR Lyrae stars were affected, but probably around 40–50 per cent of all RRab stars (Jurcsik et al. 2009; Benkő et al. 2010; Kolenberg et al. 2010). Also among RRc type stars, amplitude and phase modulation was found to be surprisingly widespread (Arellano Ferro et al. 2012).

This so-called Blazhko effect was long thought to be a periodic/regular phenomenon. Traditionally, only one Blazhko period was assigned to each modulated star, and the phenomenon was expected to repeat in every Blazhko cycle, agreeing with the widely used definition that 'the Blazhko effect is a periodic amplitude and/or phase modulation with a period of several tens to hundreds of pulsation periods'. There were several reports about changes in the Blazhko modulation of various stars (see section 5 of Guggenberger et al. 2011 for a recent summary), but those reports usually had to rely on sparse data with large gaps, so that it was impossible to say when exactly a change took place and whether it happened continuously or abruptly. The Blazhko effect was therefore still considered to be a strictly repetitive phenomenon with only some rare exceptions showing secondary modulation periods (e.g. CZ Lac; Sódor et al. 2011) or changes on very long time-scales. It was not until the availability of ultraprecise data from space missions like *CoRoT* that strong and irregular cycle-to-cycle changes of a Blazhko star were documented and that it became obvious that seemingly chaotic phenomena need to be accounted for when modelling the Blazhko effect.

While the detection of cycle-to-cycle changes in the Blazhko modulation posed a significant challenge for all classical models that required a clock-work-like behaviour, some new ideas were published. Stothers (2006) suggested that transient small-scale magnetic fields modulate the turbulent convection inside the helium and hydrogen ionization zones, a mechanism which certainly could explain subsequent Blazhko cycles of different strengths. This scenario, however, was recently tested on the basis of hydrodynamical models by Smolec et al. (2011) who found that it was not possible to reproduce all observed properties of the light curve, even when allowing a huge modulation of the mixing length. On the other hand, Buchler & Kolláth (2011) successfully modelled both regular and irregular modulations by using the amplitude equation formalism. In their models, a strange attractor in the dynamics causes chaotic behaviour. The 9:2 resonance between the fundamental mode and the ninth overtone that was found by Kolláth, Molnár & Szabó (2011) to be the reason for the recently discovered phenomenon of period doubling (Szabó et al. 2010) seems to play an important role in causing a Blazhko modulation.

We present here a study of the most extreme case detected so far: V445 Lyr (KIC 6186029). This RRab star not only shows the strongest cycle-to-cycle change found up to now, but also shows a rich spectrum of additional modes in the region between 2 and 4 $d^{-1}$. Both Fourier and O − C analyses are used to investigate the variability of the pulsation and the modulation (Section 4), and the results are compared to the case of CoRoT 105288363 in Section 6. Spectroscopy and theoretical Petersen diagrams are used to determine the fundamental parameters such as metallicity, luminosity and mass (Section 5). Additionally, the new *analytic modulation approach* for data analysis recently proposed by Benkő, Szabó & Paparó (2011) is applied to the data in Section 4.4.

## 2 BACKGROUND INFORMATION ON V445 LYR

V445 Lyr, with the coordinates RA $18^h58^m26^s$ and Dec. $41°35'49''$ (J2000), is also known as KIC 6186029, or GR244, and has a *Kepler* magnitude of $Kp = 17.4$. Two publications from the pre-*Kepler* era exist for this target: Romano (1972) found it to be variable and classified it as an RR Lyrae, and Kukarkin et al. (1973) included it into his name list of variable stars. Romano (1972) also lists the photographic brightnesses of maximum and minimum to be 15.3 and 17.3 mag, respectively, indicating a surprisingly large amplitude of 2 mag, which is much higher than the amplitude observed even during extreme Blazhko maxima in the modern data. This might at least partly be explained, however, by the difference between the observed bandpasses. Unfortunately, no details of the observations and no light curves are given, and the forthcoming paper that was announced by the author could not be found. We therefore cannot know if the observed amplitude of 2 mag is real or it is possibly due to some observational errors. No error estimations of the observations were given by Romano (1972).

Since *Kepler* data have become available, two more publications have dealt with V445 Lyr, both presenting the *Kepler* data up to Q2: Szabó et al. (2010) listed V445 Lyr as a possible candidate for the period-doubling phenomenon, and Benkő et al. (2010) already noted changes in the Blazhko modulation of V445 Lyr and reported the presence of radial overtones.

## 3 *KEPLER* PHOTOMETRY

The *Kepler* space mission was launched on 2009 March 6 into an Earth-trailing heliocentric orbit (Koch et al. 2010). Its primary purpose is the detection of Earth-sized planets in the habitable zone of solar-like stars through the transit method, which requires continuous and ultraprecise photometry of over 150 000 stars for at least 3.5 years. This is also the duration of the primary mission. *Kepler* therefore not only provides the longest continuous data sets ever observed for RR Lyrae stars, but also does so with the highest photometric precision ever obtained, as a consequence greatly improving our knowledge about stellar pulsations.

The *Kepler* spacecraft carries a Schmidt telescope with an aperture of 0.95 m and 42 science CCDs which cover a field of view of about 115 $deg^2$ (Jenkins et al. 2010). The photometric bandpass ranges from 423 to 897 nm, thus avoiding the Ca II H&K lines in the blue, and fringing due to internal reflection in the red. The *Kepler* band is therefore slightly broader than a combination of Johnson $V$ and $R$, and *Kepler* magnitudes are usually about 0.1 mag from $R$ for most of the stars (Koch et al. 2010).

Every quarter orbit, the spacecraft is rotated in order to keep the solar panels oriented towards the Sun, and the radiator that cools the focal plane towards deep space (Haas et al. 2010). Data from different quarters are denominated Q1, Q2, etc. Each of the quarters which is used here has a time base of about 90 d, except Q1 which covers about 33 d.

Each measurement is based on a 6.02 s exposure plus a 0.52 s readout time. To obtain long cadence (LC) data (29.4 min), 270 measurements are co-added; for short cadence (SC) data (1 min) nine exposures are co-added (Christiansen et al. 2011).

The time of each measurement is given in truncated Barycentric Julian Date (HJD − 240 0000), and refers to the mid-point of the measurement.

### 3.1 The V445 Lyr data set

Fig. 1 illustrates the data obtained for V445 Lyr. In this paper, we present LC data obtained in quarters 1–7, with a total time base of 588 d. Because of the loss of module 3, which happened in 2010 January, there are no data available for this target in Q5. Some smaller gaps are also present in the data as can be seen in Fig. 1. Some of them are due to unplanned safe mode events or loss of fine point control, others are caused by the regular downlinks where the spacecraft's antenna is pointed towards Earth for data transmission, and science data collection is interrupted.

*Kepler* provides light curves in two different formats: raw flux or corrected flux. The latter has been processed for planet transit search by the Pre-search Data Conditioning (PDC) pipeline which is sometimes known to remove astrophysical features and which does not preserve all stellar variability. Hence here, and for the study of variable stars in general, we make use only of the raw time series.

As the spacecraft is rotated every quarter orbit, the target falls on different CCDs after each 'roll', resulting in differences in average flux due to different sensitivity levels. Additionally, trends might occur due to image motion on the CCD or sensitivity changes. The scaling and detrending which has to be performed before starting the analysis is a delicate task especially for targets like RR Lyrae stars which have high amplitudes, long periods and changes in the amplitudes [see Celik et al. (2012) for a detailed discussion]. Here, we removed linear trends which were determined from a running average separately for every quarter, and scaled every quarter to the same mean brightness. The continuity of the upper and lower envelope of the light curve was a good indicator of correct scaling. Note that due to the gap during Q5, the continuity could not be checked there. For this reason, the scaling of the data obtained after the gap might not exactly be consistent with the scaling applied before Q5.

The scaled and detrended data that were used in this analysis are available as online material in the format displayed in Table 1 (see Supporting Information).

Fig. 1(a) shows the complete combined data set of V445 Lyr. A total of 5.5 and 3.5 Blazhko cycles were observed before and after the large gap, respectively, and 900 pulsation cycles were observed. From panel (a) it is obvious that the Blazhko effect shows strong and fast changes, with almost all observed cycles having a different appearance. Panel (b) compares in a phase diagram directly a light curve from a Blazhko maximum with one obtained during the subsequent Blazhko minimum, illustrating the extremely low pulsation amplitude that occurs during some, but not all, modulation minima. Note that due to the very small amplitude and the distorted light curve showing a double maximum (see also Fig. 1d) it would not be possible to recognize the RR Lyrae nature of this star when

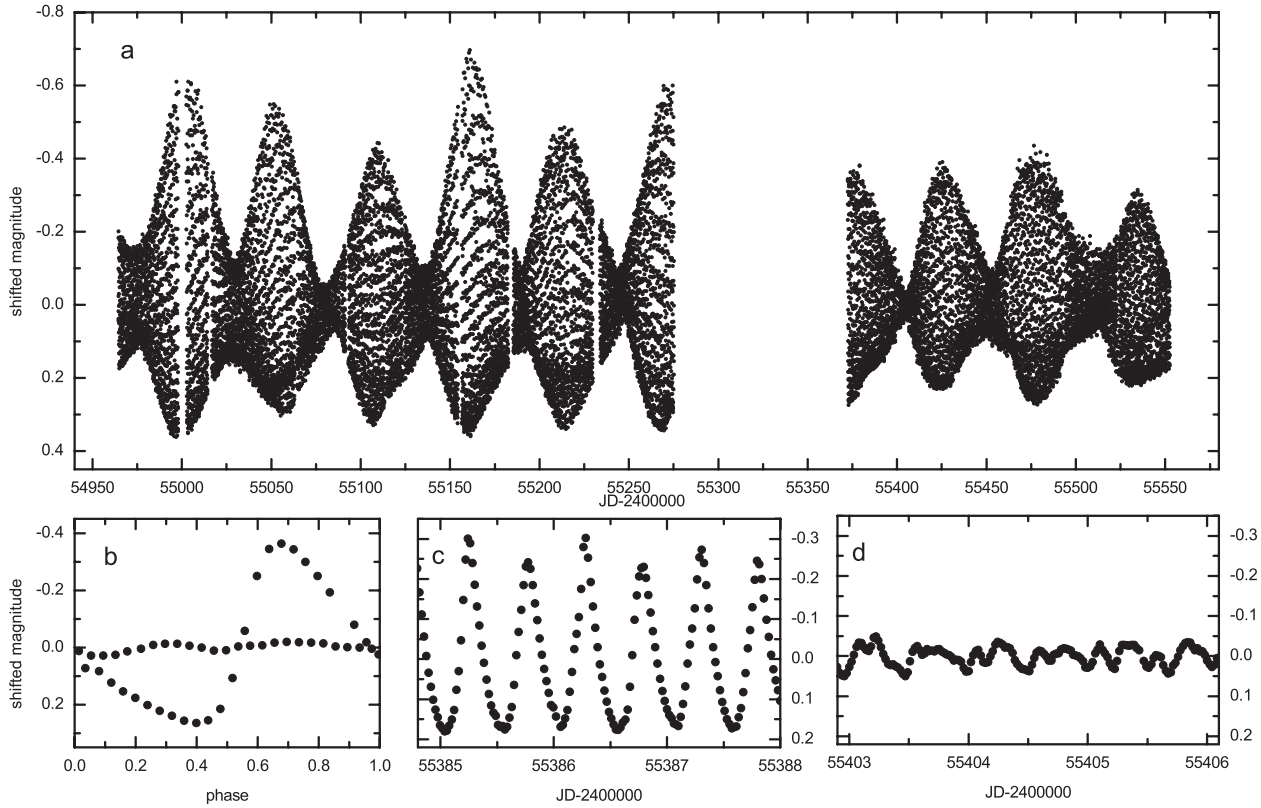


**Figure 1.** Panel (a) shows the complete light curve of V445 Lyr presented in this paper, including quarters Q1–Q7. Due to failure of a module, there are no data from Q5, resulting in the gap from MJD 55273 to 55372. Panel (b) illustrates the extreme Blazhko modulation by comparing a pulsation cycle at Blazhko maximum to one at Blazhko minimum. The light variation has an extremely low amplitude during this Blazhko minimum and shows a double maximum. In panel (c), a zoom into a region with period doubling is shown as an example and panel (d) emphasizes the distorted light-curve shape that occurs during some Blazhko minima.

**Table 1.** The scaled and detrended data set of V445 Lyr that was used for the analysis in this paper. Column 1 gives the truncated Barycentric Julian Date, column 2 gives the magnitude with the average shifted to zero and column 3 gives the quarter in which data were obtained. The full table is available as Supporting Information with the online version of the paper.

| HJD − 240 0000 | Magnitude | Quarter |
|---|---|---|
| 54964.512 11 | 0.044 188 798 | Q1 |
| 54964.532 54 | 0.038 912 686 | Q1 |
| 54964.552 98 | 0.017 979 982 | Q1 |
| 54964.573 41 | −0.023 960 246 | Q1 |
| 54964.593 85 | −0.099 222 117 | Q1 |
| ... | ... | ... |

observing it only during Blazhko minimum where the peak-to-peak amplitude can be as low as 70 mmag. Extremely low pulsation amplitudes during Blazhko minima were recently also reported by Sódor et al. (2012) for two of the RRab type stars, and the occurrence of a strong bump during Blazhko minimum was noted in RZ Lyr (Jurcsik et al. 2012). In Fig. 1(c), a small part of the light curve around JD 245 5386 is shown, illustrating the phenomenon of period doubling (alternating higher and lower light maxima) which was recently discovered in *Kepler* Blazhko stars (Szabó et al. 2010) and which is also present in V445 Lyr.

## 4 ANALYSIS AND RESULTS

Due to the quasi-continuous coverage and the high photometric precision, the conditions for a Fourier analysis are more than favourable. The spectral window function (see Fig. 2) is almost perfect, without any alias peaks visible at first glance. Because of the Earth-trailing orbit, no orbital frequencies like the ones that cause trouble in the data from many other space missions are present here.

A well-known feature in the *Kepler* data is the momentum desaturation of the reaction wheel, which happens every 2.98 d. During the thruster firings which are necessary to release the angular momentum that has built up in the reaction wheels, the spacecraft momentarily loses the fine point control (Van Cleve & Caldwell 2009). This results in a missing data point during every desaturation in the otherwise regularly spaced data, leading to a comb-like structure in the Fourier transform with a spacing of 0.335 $d^{-1}$. In the spectral window, those peaks have a very low normalized amplitude of only 0.004 mag. A zoom into the spectral window (see lower panel of Fig. 2) reveals this comb of tiny peaks. When carefully removing all high-amplitude peaks from the Fourier spectrum before turning to interpreting features with amplitudes which are orders of magnitude smaller as discussed in Section 4.1.5, those alias peaks are not expected to cause any trouble.

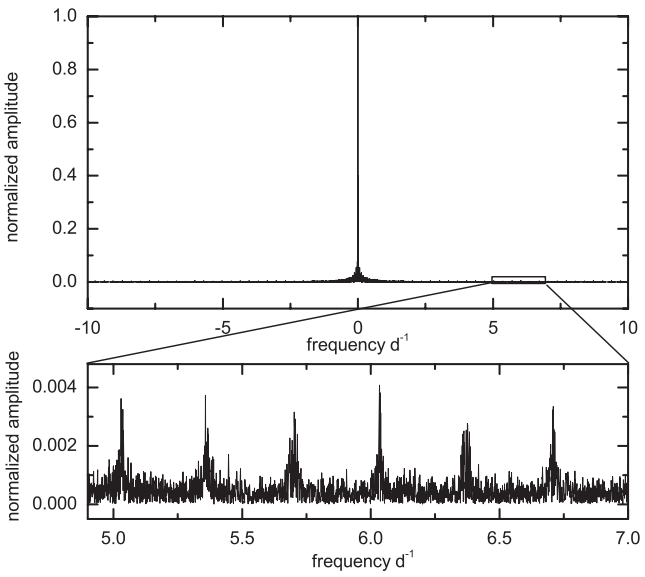


**Figure 2.** Spectral window function of the complete V445 Lyr data set. Lower panel: magnification of the region between 5 and 7 $d^{-1}$, showing some examples of the low-amplitude features caused by the reaction wheel.

Other features in the spectral window function are two harmonics of the monthly data downlink frequency, at 0.065 and 0.13 $d^{-1}$, with normalized amplitudes of 0.05 and 0.03 mag, respectively.

Due to the time base of 588 d, the Rayleigh frequency resolution is 0.0017 $d^{-1}$.

### 4.1 Fourier analysis of the full data set

As a first step, a Fourier analysis of the complete data set was performed, keeping in mind that changes in the fundamental period might occur during the time of the observations and that the changes of the Blazhko modulation cause a large number of peaks close to the classical pulsation and modulation components. The Fourier analysis of the full data set, however, is necessary to obtain an overall picture of the pulsation and modulation properties of V445 Lyr to find the mean values of the pulsation and modulation periods and to detect possible long-term periodicities which can be resolved with a long time base only.

The Fourier analysis of the complete data set was performed with PERIOD04 (Lenz & Breger 2005) and then checked with SIGSPEC (Reegen 2007). The results agreed within the errors. The Fourier analysis revealed a mean pulsation period of 0.513 075 ± 0.000 005 d and a mean Blazhko period of 53.1 ± 1 d with the ephemeris

$$\mathrm{HJD}(T_{\mathrm{max,pulsation}}) = 245\,5550.514 + 0.513\,075 E_{\mathrm{pulsation}},$$

$$\mathrm{HJD}(T_{\mathrm{max,Blazhko}}) = 245\,5534.2 + 53.1 E_{\mathrm{Blazhko}}.$$

Note that the presence of close peaks has a great influence on the fitting and frequency optimization procedure, and the errors are therefore larger than would normally be expected for a Fourier fit to data of the given quality.

#### *4.1.1 Multiplet components*

The Blazhko multiplets (i.e. the pattern of peaks which is typical for Blazhko stars with peaks at the positions $kf_0 \pm nf_B$, with $k$ and $n$ being integers denoting the harmonic order and the multiplet order, respectively, and with $f_0$ and $f_B$ denoting the fundamental and the Blazhko frequency) were found to be very asymmetric in amplitude. Much higher amplitudes appeared on the right-hand (higher frequency) side than on the left. This is the more common case, which is observed in three-fourths of all Blazhko RRab stars (Alcock et al. 2003). Components were detected up to quintuplet order on the right-hand side, while on the left-hand side of the main pulsation component only one side peak (i.e. a triplet component, $n = 1$) could be found. In some orders, peaks were found near the positions that would be expected for septuplets, but the deviations

from the exact frequency values were considered too big to identify the peaks safely as septuplet components.

In addition to the classical Blazhko multiplets around the fundamental mode and its harmonics, a secondary modulation component, $f_S$, could also be identified. It manifests itself as a series of additional peaks next to the classical modulation side peaks of the Fourier spectrum, appearing in every order with a spacing of $0.006\,98 \pm 0.000\,27\,d^{-1}$, indicating a secondary modulation period of $143.3 \pm 5.8$ d. The secondary peaks appearing on the right-hand side of the classical peaks show surprisingly high amplitudes, while the secondary peaks to the left of the classical multiplet have small amplitudes and could only be detected after pre-whitening a large number of higher amplitude peaks. Interestingly, the peaks belonging to this additional series could also be detected at higher multiplet orders ($n = 3$) than the classical multiplet, making it difficult to explain the peaks as combination frequencies. Their amplitudes seem to decrease less quickly with increasing harmonic order $k$ (see also Section 4.1.3), making them easier to spot at high orders.

Fig. 3 shows the Fourier transform of the data, providing also zooms into the regions around the third, fourth and fifth harmonic order where both the classical multiplet and the additional components can be seen. The highest peaks among the multiplet components, which can be seen even before pre-whitening the original data, are marked with arrows.

Fig. 4 illustrates the pattern of detected frequencies in the vicinity of the fundamental pulsation and its harmonics in the style of an 'echelle' diagram. In this diagram, which is similar to the diagrams used to unveil equally spaced peaks in helioseismology, the frequency of each peak is plotted against ($f$ modulo $f_0$), i.e. $f/f_0 - \mathrm{INT}(f/f_0)$ or $f/f_0 - \mathrm{INT}(f/f_0) - 1$ for peaks to the left of the harmonic, therefore clearly revealing patterns which repeat in every harmonic order. Peaks belonging to the same group of combinations align in vertical ridges. We stress that unlike in the helioseismic application, where the ridges denote different radial orders of same degree, in this case the echelle diagram only serves the purpose of displaying in a very practical and easy way the repeating patterns in different harmonic orders of non-sinusoidal fundamental radial pulsation.

### *4.1.2 Deviation of the harmonics*

Due to the non-sinusoidal light-curve shape typical for RR Lyrae stars, harmonics of the fundamental mode are expected to appear at frequencies $kf_0$, where $k$ is an integer denoting the harmonic order. The classical Blazhko multiplets in the modulated stars are spaced equidistantly, implying frequency values of $kf_0 \pm nf_B$ with $n$ denoting the multiplet order. Long-term period changes and close peaks caused by irregular phenomena, however, can distort this frequency pattern. When analysing time series of Blazhko RR Lyrae stars, there are two options for fitting the data: one is to fix the frequencies of the harmonics and Blazhko multiplets to their expected values of $kf_0 + nf_B$, thereby reducing the number of free parameters in the fit. The other option is to let all parameters, including the frequency values, free. When the latter option was applied to this data set, the harmonics were observed to deviate systematically and significantly from their expected values, which can also be noticed as a slight rightwards tilt of the ridges in the echelle diagrams (Fig. 4). Normally, one would expect that this is simply caused by a wrong value of $f_0$, but in this case, no value of $f_0$ could be found which could solve the issue, i.e. every detected harmonic, when divided by its order, required a different $f_0$. We therefore decided in favour of

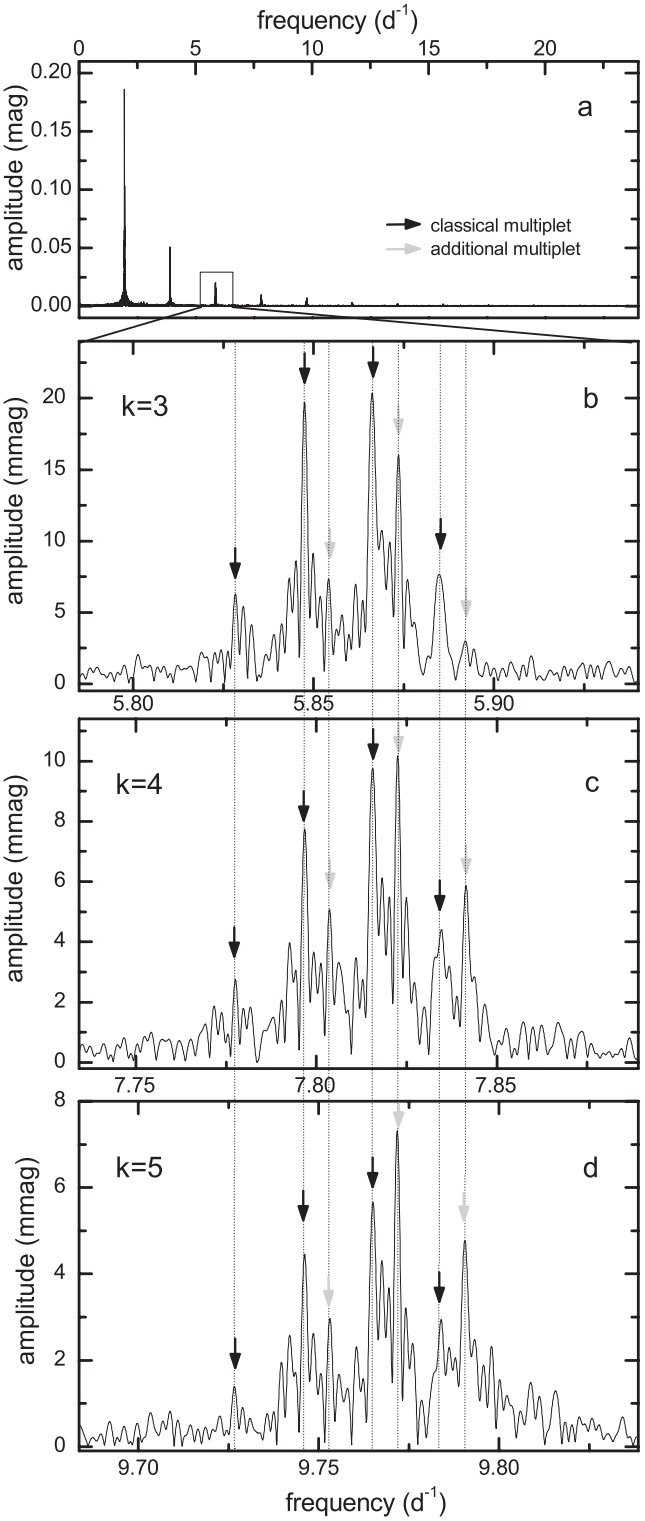


**Figure 3.** Fourier transform of the complete V445 Lyr data set (upper panel). In the lower panels (b, c and d), the regions around the harmonics $kf_0$ with $k = 3$, 4 and 5 are shown in detail. Black arrows indicate the peaks belonging to the classical Blazhko multiplet with $kf_0 - f_B$, $kf_0$, $kf_0 + f_B$ and $kf_0 + 2f_B$, while grey arrows indicate some of the peaks belonging to the secondary multiplet which within itself has a spacing equal to the Blazhko frequency, but is shifted with respect to the classical multiplet by $0.006\,98\,d^{-1}$. Note that from order $k = 4$ onwards, the highest amplitude peak in this order is a peak belonging to the secondary multiplet.

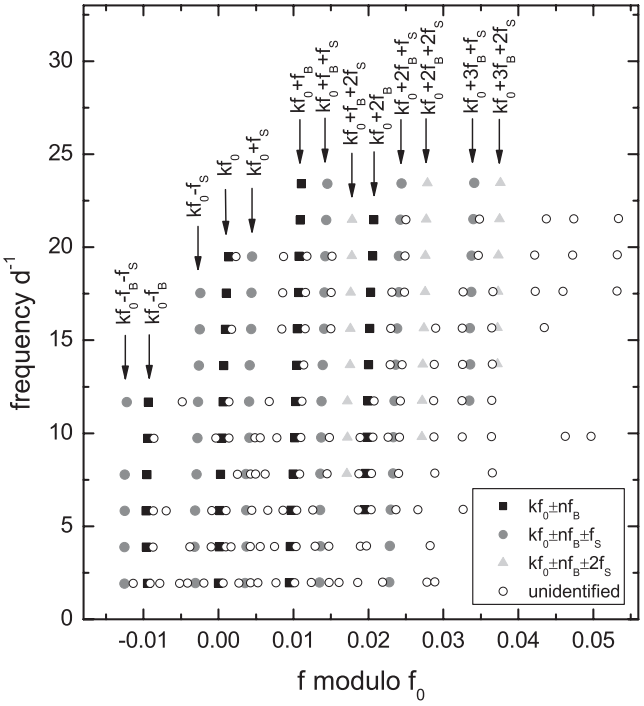


**Figure 4.** 'Echelle' diagram of the peaks detected in the vicinity of the fundamental pulsation mode and its harmonics. Frequency is plotted versus $f$ modulo $f_0$, so that regularly spaced peaks which appear in every order align in vertical patterns, making it easy to identify combinations with $f_0$. Peaks belonging to the category $kf_0 \pm nf_B$ are shown as black squares, peaks of the group $kf_0 \pm nf_B + f_S$ are shown as grey circles and components of $kf_0 + nf_B + 2f_S$ are plotted with light-grey triangles. Open circles denote unidentified and/or unresolved peaks, some of which originate from the non-repetitive nature of the modulation and long-period changes.

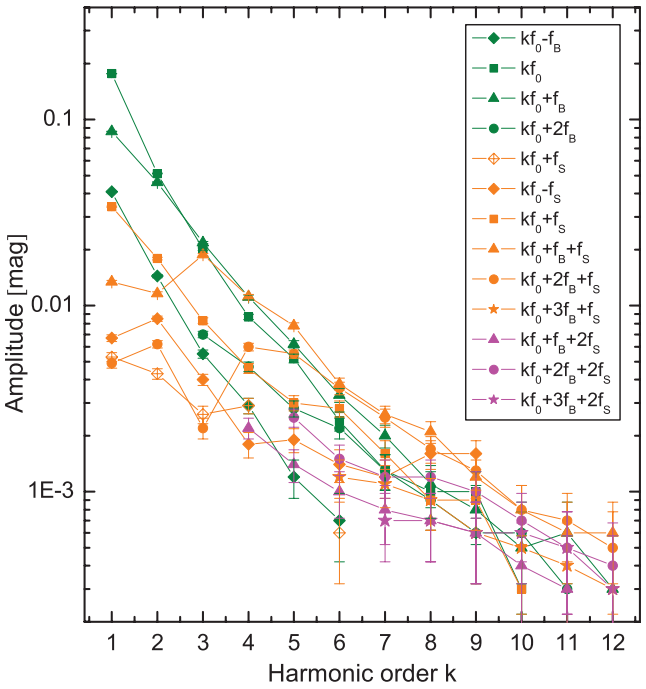


**Figure 5.** Amplitudes of all components versus harmonic order. Components belonging to the classical Blazhko multiplet are shown with green symbols, peaks which are combinations with $f_S$ are shown in orange, and components with a $2f_S$ term are shown in magenta. It can be seen that the amplitude of the $f_S$ multiplets decrease less steeply than those of the classical Blazhko multiplet, reaching the same amplitude in the fourth order and dominating the frequency spectrum for higher orders.

the more pure approach and did not fix the frequency values to the expected positions, but left all parameters free in the fit of the complete data set. The problem disappeared, however, when analysing different subsets of data separately (see Section 4.2), and we therefore suspect it to be either the result of period changes which take place during certain seasons (see also Section 4.3) and/or close unresolved peaks which are known to strongly influence the results of both the Fourier analysis and the multisine fitting procedure.

### *4.1.3 Amplitudes versus harmonic order*

It is a well-known fact that in Blazhko RRab stars the amplitudes of the multiplet side peaks decrease less rapidly with harmonic order than that of the main component. This was first described by Jurcsik et al. (2005), and then confirmed for other well-studied stars such as SS For (Kolenberg et al. 2009), RR Lyr (Kolenberg et al. 2011) and CoRoT 105288363 (Guggenberger et al. 2011). As expected, the result is the same for V445 Lyr (see Fig. 5), but in an extreme way with the amplitude of the right-hand side peak exceeding that of the main component as early as in the third order. Additionally, the amplitudes of the secondary modulation multiplet, i.e. combinations with the secondary modulation $f_S$, could be studied in this case. It turned out that the amplitudes of the secondary multiplet components decrease even less steeply, therefore dominating the Fourier spectrum from the fourth order onwards. The strongest signal then comes from the combination $f_0 + f_B + f_S$, i.e. the peak on the right-hand side of the right triplet component. Also, combinations with the term $2f_S$ could be detected, and their amplitudes are plotted in Fig. 5. They also show a very slow amplitude decrease.

### *4.1.4 Number of relevant frequencies*

Due to the dense spectrum of peaks which is caused by the cycle-to-cycle changes of the Blazhko effect, an analysis in the classical sense, i.e. taking into account all frequencies down to a certain signal-to-noise ratio level or a certain significance criterion, might not be optimal in a case like V445 Lyrae, as it does not yield meaningful results. A large number of the detected peaks is likely to be the result of 'stellar noise' caused by irregular and/or long-periodic phenomena, and many of them are not resolved with the available time span. Tests revealed that as many as 771 frequencies can be found when performing an analysis until the generally adopted criteria of significance are reached. Many of them were not resolved, and many could not be attributed to any combination of other modes, and did not show repeating patterns in the echelle diagrams. Therefore, instead of choosing the classical approach, the analysis was stopped after a certain number of the highest peaks in every harmonic order were found and pre-whitened, usually around 20 peaks per order. It turned out that after subtracting approximately 20 peaks in a given harmonic order, no meaningful combinations could be identified among the following peaks, and many unresolved peaks appeared. In Fig. 4 only the highest peaks of every order are shown, already including some unresolved peaks which could not be avoided due to their high amplitudes. As the Nyquist frequency of LC data is 24.4 d$^{-1}$, 12 harmonic orders could be observed, and 239 frequencies were subtracted around the main pulsation components until the attention was turned towards the additional peaks which are

present in the region between the harmonics of the fundamental mode (see the next section).

Altogether, 239 frequencies were included, of which one is the fundamental mode, nine are harmonics of the fundamental mode, 104 are combinations of $f_0$ or its harmonics with the Blazhko frequency $f_B$ and/or the secondary modulation $f_S$ and 125 are unidentified.

### *4.1.5 Additional frequencies: radial overtone and non-radial pulsation*

It was already noted by Benkő et al. (2010) that V445 Lyr shows a rich spectrum of frequencies in the region between the harmonics of the fundamental mode. Those frequencies are not at all typical for ab-type RR Lyrae stars and have never been detected in such a large number in an RR Lyrae star. Some peaks were suspected to be radial overtones by Benkő et al. (2010), and also frequencies which are half-integer multiples of the fundamental mode are expected to appear in this region as a consequence of the period-doubling phenomenon as described by Szabó et al. (2010). However, there is more than this in the case of V445 Lyr.

Fig. 6 shows the frequency spectrum after subtraction of the relevant peaks around the multiples of the fundamental pulsation as discussed in the previous section (their former positions are marked with arrows). The additional frequencies can clearly be seen to be the dominant signal with an amplitude of 3.7 mmag for the highest peak. The region between the fundamental mode and its first harmonic is indicated with a grey box and enlarged in the insert (panel b). Four frequency regions with enhanced signal can be noted in the enlargement: around 2.65, 2.8, 2.9 and 3.33 $d^{-1}$. This pattern repeats in every harmonic order, indicating combinations of the frequencies with the fundamental mode and its surrounding peaks. The presence of combinations is a strong evidence that the additional signal is not introduced by a possible background star.

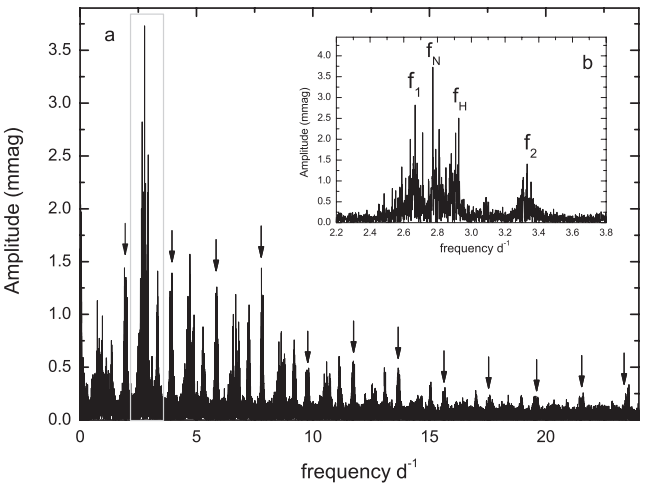


**Figure 6.** Fourier spectrum after pre-whitening 239 frequencies in the vicinity of the fundamental mode and its harmonics. Very clearly, additional frequencies can be seen between the harmonic orders and their combinations with $f_0$ which are present up to high harmonic orders. Arrows mark the places where the harmonics and the Blazhko as well as the secondary multiplets were located before pre-whitening. Some signal remains around their positions, as discussed in Section 4.1.4. The insert (panel b) shows a zoom into the region between the fundamental mode and the first harmonic (2–4 $d^{-1}$), indicated as a grey square.

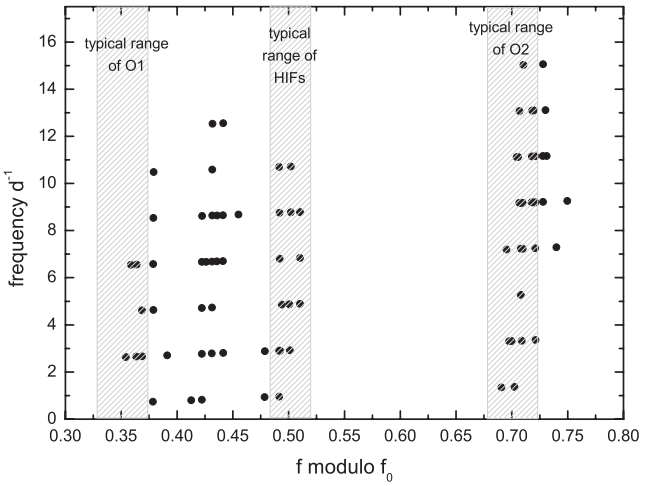


**Figure 7.** Echelle diagram of the additional frequencies, showing how the patterns repeat in every harmonic order. Shaded boxes indicate the ranges which would be typical for the first and second overtones (O1 and O2, respectively), as well as for the HIFs.

In a Fourier analysis of the relevant frequency regions, 80 peaks (including combinations) were considered significant and were subtracted. A closer inspection of the result revealed that the dominant peaks formed combinations not only with the fundamental mode but also with the Blazhko multiplet peaks (including quintuplets!) and in some cases also with the peaks belonging to the secondary multiplet. Negative combinations such as $f_N - f_0 - f_B$ also occur. Significant combination peaks can be traced up to the fifth harmonic order, but an excess in signal is visible in the Fourier spectrum even at much higher orders (see Fig. 6). In Fig. 7, an echelle diagram is plotted for the additional peaks, clearly showing the combinations with the fundamental mode aligned in vertical patterns. Shaded boxes indicate the typical regions in which overtone modes and half-integer combination frequencies would be expected to be situated. Please note that it was shown by Szabó et al. (2010) that due to the onset and offset of the period-doubling phenomenon, the half-integer frequency (HIF) peaks are not necessarily located at the exact positions of the half-integer multiples, but might deviate by several per cent. Therefore, the shaded box at ($f$ modulo $f_0$) = 0.5 in Fig. 7 has a distinct width.

In V445 Lyr, the frequency at 2.9256 $d^{-1}$ deviates by only 0.0021 $d^{-1}$ (i.e. 0.07 per cent) from the exact value of $3f_0/2$. Given the fact that clear signs of period doubling are indeed visible in the light curve (see Fig. 1c), and considering the above-mentioned findings of Szabó et al. (2010), it is quite safe to interpret this frequency as an HIF caused by period doubling. We hereafter refer to it as $f_H$. Four significant HIFs (which can also be interpreted as combinations of $f_H$ with $f_0$) were found in the Fourier spectrum: $3f_0/2$, $5f_0/2$, $9f_0/2$ and $11f_0/2$. Combinations with the Blazhko frequency, both positive and negative, could also be identified (see Table 2 for a complete list).

Another interesting feature is the peak at 3.3307 $d^{-1}$ which shows a frequency ratio of $f_0/f_2 = 0.585$ with the fundamental mode, and which we hereafter refer to as $f_2$. Its period ratio is typical for the second overtone. Peaks with similar period ratios have already been reported for several RR Lyrae stars. Poretti et al. (2010) were the first to find them in the star CoRoT 101128793. The frequency ratio in their study was 0.584 with the fundamental mode at $f_0 = 2.11895\,d^{-1}$. They interpreted the peak as the second radial overtone. The same authors also re-analysed the data of V1127

**Table 2.** List of the highest peaks in every one of the four regions of excess signal, and their combinations.

| | Frequency ($d^{-1}$) | Amplitude (mmag) |
|---|---|---|
| $f_N$ | 2.7719 | 3.67 |
| $f_N + f_0$ | 4.7211 | 1.58 |
| $f_N + 2f_0$ | 6.6778 | 0.74 |
| $f_N + 3f_0$ | 8.6196 | 0.51 |
| $f_N - f_0$ | 0.8228 | 0.75 |
| $f_N + f_B$ | 2.7895 | 1.64 |
| $f_N + f_0 + f_B$ | 4.7389 | 1.43 |
| $f_N + 2f_0 + f_B$ | 6.6880 | 1.22 |
| $f_N + 3f_0 + f_B$ | 8.6372 | 0.83 |
| $f_N + 4f_0 + f_B$ | 10.5864 | 0.54 |
| $f_N + 5f_0 + f_B$ | 12.5359 | 0.33 |
| $f_N - f_0 - f_B$ | 0.8044 | 0.69 |
| $f_N + 2f_B$ | 2.8091 | 2.24 |
| $f_N + 2f_0 + 2f_B$ | 6.7067 | 0.87 |
| $f_N + 3f_0 + 2f_B$ | 8.6559 | 0.57 |
| $f_N + 5f_0 + f2f_B$ | 12.5543 | 0.34 |
| $f_N + 2f_0 + f_S$ | 6.6778 | 0.74 |
| $f_N + 2f_0 + f_B + f_S$ | 6.6964 | 0.76 |
| $f_N + 3f_0 + f_B + f_S$ | 8.6456 | 0.81 |
| $f_N + 3f_0 + 3f_B + f_S$ | 8.6828 | 0.53 |
| $f_1$ | 2.6676 | 2.80 |
| $f_1 + f_0$ | 4.6166 | 1.08 |
| $f_1 + f_0 + f_B$ | 4.6362 | 1.16 |
| $f_1 + 2f_0 + f_B$ | 6.5851 | 1.02 |
| $f_1 + 3f_0 + f_B$ | 8.5343 | 0.77 |
| $f_1 + 4f_0 + f_B$ | 10.4838 | 0.45 |
| $f_1 - f_0 + f_B$ | 0.7374 | 1.16 |
| $f_H$ | 2.9256 | 2.55 |
| $f_H + f_0$ | 4.8736 | 0.87 |
| $f_H + 3f_0$ | 8.7743 | 0.60 |
| $f_H + 4f_0$ | 10.7234 | 0.43 |
| $f_H - f_B$ | 2.9070 | 2.29 |
| $f_H + f_0 - f_B$ | 4.8607 | 0.89 |
| $f_H + 2f_0 - f_B$ | 6.8060 | 0.95 |
| $f_H + 3f_0 - f_B$ | 8.7549 | 0.57 |
| $f_H + 4f_0 - f_B$ | 10.7029 | 0.40 |
| $f_H - f_0 - f_B$ | 0.9579 | 1.01 |
| $f_H + f_0 + f_B$ | 4.8924 | 1.00 |
| $f_H + 2f_0 + f_B$ | 6.8413 | 0.71 |
| $f_H + 3f_0 + f_B$ | 8.7905 | 0.58 |
| $f_2$ | 3.3307 | 1.43 |
| $f_2 + f_0$ | 5.2781 | 0.85 |
| $f_2 + 2f_0$ | 7.2268 | 0.79 |
| $f_2 + 3f_0$ | 9.1760 | 1.04 |

Aql (Chadid et al. 2010) and MW Lyr (Jurcsik et al. 2008) and found frequency ratios of 0.582 ($f_0 = 2.8090 d^{-1}$) and 0.588 ($f_0 = 2.5146 d^{-1}$), respectively. In the sample of *Kepler* RRab stars, Benkő et al. (2010) reported the presence of the second overtone in four different stars: V354 Lyr (a Blazhko star with $f_0 = 1.780\,37 d^{-1}$), V2178 Cyg (a Blazhko star with $f_0 = 2.054\,23$), V445 Lyr (the subject of this paper) and the non-modulated RRab star V350 Lyr ($f_0 = 1.682\,82$) which was the first example of a non-Blazhko double-mode RR Lyrae star with the fundamental (F) and the second overtone (O2) excited. Guggenberger et al. (2011) found evidence for the second overtone in CoRoT 105288363, a Blazhko star with rapid changes in the Blazhko effect, and Nemec et al. (2011) found the second overtone in KIC 7021124, therefore providing another example of a non-modulated RRab star pulsating in both F and O2 ($f_0 = 1.606\,445 d^{-1}, f_0/f_2 = 0.593$).

It is interesting to note how different the stars are for which the second overtone has been documented so far: their fundamental frequencies range from about 1.6 to 2.8 $d^{-1}$, covering almost the full bandwidth of RRab pulsation, and with respect to stability they range from non-modulated stars with almost perfectly regular RRab pulsation (V350 Lyr, KIC 7021124) to Blazhko stars with a rather regular Blazhko effect (CoRoT 101128793 and V1127 Aql) and finally to modulated stars that show dramatic changes of their Blazhko modulation (CoRoT 105288363 and V445 Lyr). Moreover, they cover a significant range of Blazhko periods, from 16.6 d to more than 200 d, as estimated for V2178 Cyg.

The combinations of $f_2$ in V445 Lyr deserve some special attention. While as many as 32 peaks are detected near the positions of $f_2 + kf_0$, and clearly an excess of signal is visible in every harmonic order (see Figs 6 and 7), it was not possible to identify most of the detected peaks as exact combinations with the known frequencies. For $f_H$ (which was discussed in the previous paragraph), 12 out of 16 peaks could be attributed to combinations while for $f_2$, only three combinations with $f_0$ were found at their exact positions. All the other peaks in the vicinity of the combinations deviated too much from the calculated values to be safely matched with the combinations. This is especially remarkable as the amplitudes of those peaks are surprisingly large in higher harmonic orders compared to the combinations of the other additional frequencies. From Fig. 6 it is obvious that in the first harmonic order, $f_2$ has a small amplitude compared to the other additional frequencies, while at the orders 4–5 they become equal, and at higher orders, the peaks in the area around $f_2 + kf_0$ are the dominant features. This is also illustrated in Fig. 8, where the amplitudes of the safely identified peaks versus frequency are shown. The large number of unidentified peaks around $f_2$ might indicate that the amplitude of $f_2$ is variable, either irregularly or on a time-scale other than the Blazhko frequency. This will be discussed in more detail in Section 4.2.1.

The highest amplitude peak among the additional frequencies (3.7 mmag) is the one at 2.7719 $d^{-1}$. This peak was interpreted as the first overtone by Benkő et al. (2010), but its ratio with the

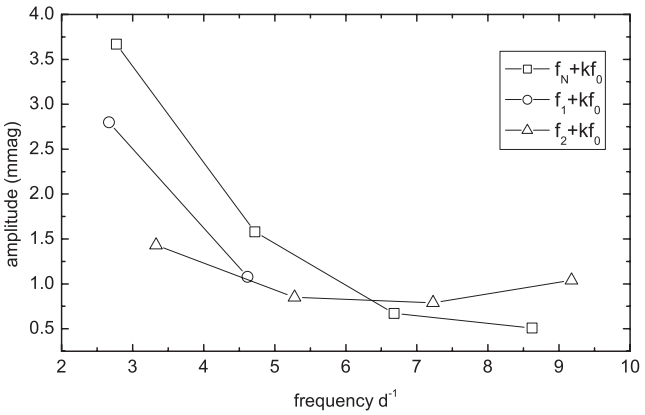


**Figure 8.** Amplitudes of the additional frequencies and their combinations with $f_0$ versus frequency. While the amplitudes of $f_N$ and $f_1$ decrease exponentially with harmonic order, the amplitude of $f_2$ remains almost stable. Amplitude errors are smaller than the symbols.

fundamental ($f_0/f_N = 0.703$) is very low compared to the canonical value of 0.74–0.75. Note that the OGLE III RR Lyrae stars in the Galactic bulge have $f_0/f_1$ values going down to about 0.726 only (see Soszynski et al. 2011). Extremely high metallicity values would be necessary according to models (Popielski, Dziembowski & Cassisi 2000; Szabó, Kolláth & Buchler 2004; Smolec & Moskalik 2008) to fit this frequency ratio with the first overtone. New spectroscopic results revealed, however, that the metallicity of V445 Lyr is [Fe/H] $= -2.0 \pm 0.3$ (see Section 5), rendering it impossible to explain this frequency with a radial overtone mode. $f_N$ is therefore most likely to be a non-radial mode. We note that Van Hoolst, Dziembowski & Kawaler (1998) found in their non-adiabatic and non-radial calculations the excitation of non-radial modes in the vicinity of the radial mode in RR Lyrae stars to be very likely, and Dziembowski & Cassisi (1999) noted in their model survey the presence of strongly trapped non-radial modes with very high growth rates near the first overtone.

Among the additional modes in V445 Lyr, $f_N$ is the one that shows the clearest pattern of combination frequencies: of 20 peaks which were found significant in relation to $f_N$, all 20 could be unambiguously identified as exact combinations with $f_0$, the Blazhko frequency and the secondary modulation frequency (see also Table 2 and Fig. 9, which illustrate the regular pattern of combination peaks). We note that the possible non-radial mode, which was found by Chadid et al. (2010) in V1127 Aql, has a very similar frequency ratio (0.696), may be hinting at a possible systematic preference in non-radial mode excitation in RR Lyrae stars.

There remains, however, the fourth region of increased signal with a main peak at 2.6676 d$^{-1}$, which, with a frequency ratio of $f_0/f_1 = 0.731$ is in principle in the possible range of the first overtone pulsation. One has to note that double-mode RR Lyrae stars usually follow a well-defined empirical sequence in the Petersen diagram; in other words, there is a relation between $f_0$ and $f_0/f_1$ (see Popielski et al. 2000; Soszynski et al. 2009). If the peak at 2.6676 d$^{-1}$ is indeed the first overtone, V445 Lyr would be an exception to this relation, which is very unlikely. On the other hand, outliers from the sequence similar to V445 Lyr have recently been reported by Soszynski et al. (2011) in the OGLE III survey of the Galactic bulge.

The metallicity needed to reproduce a frequency ratio of $f_0/f_1 = 0.730$ with models ($Z = 0.004$, see Fig. 10) is much larger than the spectroscopic value ($Z = 0.0002$, see also Section 5). Moreover, the average frequency values are quite far ($2f_1 - f_0 - f_2 = 0.055$) from the resonance condition that could explain the presence of the second overtone by resonant excitation, and which would also have the power to shift the frequency away from the expected value in the Petersen diagram. We note, however, that the frequency values of $f_1$ and $f_2$ are not strictly constant during the observed time span, but undergo irregular fluctuations. We performed a time-dependent Fourier analysis (see also Section 4.2.1) and found the resonance criterion to be fulfilled occasionally. For $f_1$, one combination with $f_0$ and five combination frequencies with $f_0$ and $f_B$ were found, leaving the other six significant peaks unidentified. One of them, a peak at 2.639 d$^{-1}$ (with a frequency ratio of 0.739 with the fundamental mode), would fulfill the resonance criterion, but its amplitude is only 1.9 mmag, compared to 2.8 mmag of $f_1$. We therefore conclude that the identities of the peaks at 2.6676 and 2.639 d$^{-1}$ cannot be unambiguously assessed.

The highest peaks in every region and their combinations are listed in Table 2. Altogether, 80 frequencies were found to be significant in the vicinity of the additional peaks: four of these were independent frequencies, 40 were combinations of these independent terms with $f_0$, $f_B$ and/or $f_S$, and 36 were peaks which could not be identified as combinations. Together with the 239 frequencies found in the vicinity of the fundamental mode and its harmonics (see Section 4.1.4), this results in a total of 319 frequencies included in the analysis.

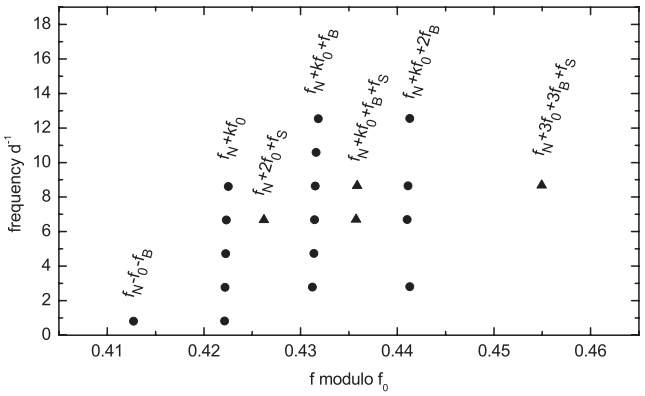


**Figure 9.** Details of the echelle diagram, showing only the vicinity of the mode $f_N$. All detected peaks could clearly be identified as combinations of $f_N$ with either the classical Blazhko multiplet or the secondary multiplet. The fact that no unidentifiable peaks are among the highest ones points towards a very stable amplitude of this mode, compared to the other additional peaks that were found in this star.

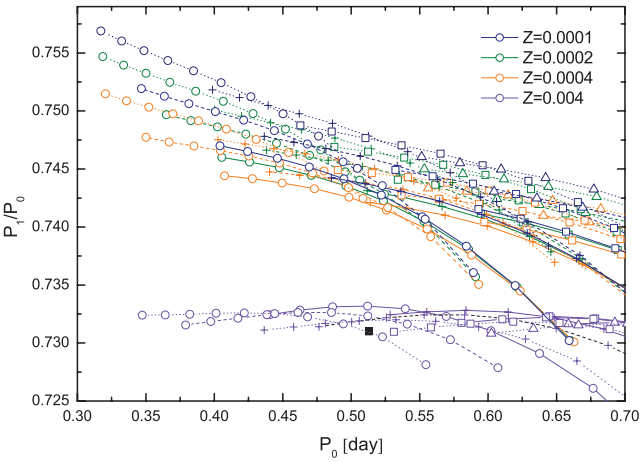


**Figure 10.** Petersen diagram for the peak at 2.6676 d$^{-1}$ illustrating that a metallicity of $Z = 0.004$ would be necessary to identify this peak as the first radial overtone mode. Models around the spectroscopically derived value of $Z = 0.0003$ (see Section 5) are also shown for comparison. Different symbols indicate different luminosities and different line styles indicate different masses (see also Section 5). Models were calculated with the Warsaw codes (Smolec & Moskalik 2008).

### 4.2 Separate analysis of subsets

To study the time-dependent behaviour of the frequency pattern, we used both PERIOD04 and the *time-resolved* feature of SIGSPEC (Reegen 2007), which makes it possible to analyse large numbers of data subsets in an automated way. The top panel of Fig. 11 illustrates the variation of $f_0$ with time as calculated with SIGSPEC for overlapping subsets of 15 d. With PERIOD04, we analysed larger subsets of data, consisting of one or more quarters each. During this process we note that in the subset containing Q1 to Q4 (Blazhko period 53.9 d), no

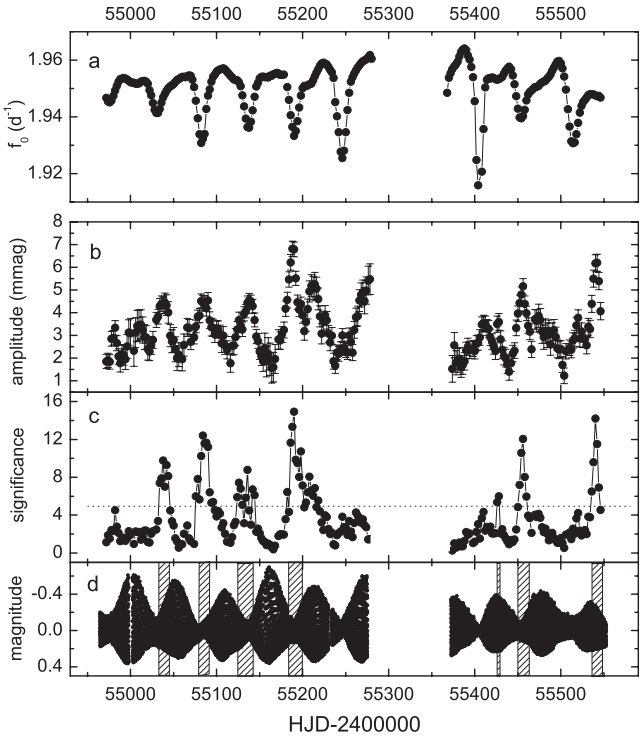


**Figure 11.** Variation of $f_0$ over the complete data set (panel a). Middle panels show the variation of the amplitude (panel b) and the significance (panel c) of the second overtone $f_2$, calculated for bins of 15 d duration with a step width of 2 d. The bottom panel (d) shows the light curve for orientation. The times of significant $f_2$ amplitude are marked with shaded boxes.

deviation of the harmonics as described in Section 4.1.2 is observed. This phenomenon seems to occur only in quarters Q6 and Q7 where the Blazhko periods found in separate analyses of the quarters were 79.8 and 80.4 d, respectively.

### 4.2.1 *Stability of the additional frequencies*

The results discussed in Section 4.1.5 hint towards a variability of the amplitude of $f_2$, and we therefore studied the temporal evolution of this peak in detail. Using the time-resolved mode of SigSpec, we performed a Fourier analysis of overlapping bins with a duration of 15 d in steps of 2 d, limiting the frequency range to the region around $f_2$. The resulting amplitudes are plotted in Fig. 11(b). While there is a clear variation of the amplitude ranging from 2 to ∼7 mmag, no clear periodicity is discernible. We also performed a Fourier analysis on the resulting amplitude curve and found no significant frequency of variability. We note that in Fig. 11, all values of $A(f_2)$ were included, regardless of the significance of the frequency. Only bins with an insufficient number of data points and/or bad frequency resolution were discarded. Therefore we provide as a supporting plot the time-dependent significance of the peaks in panel (c), where the most commonly used significance criterion of sig $\geq 5$ is indicated with a dashed line.

For better orientation, the bottom panel shows the full data set (light curve) of V445 Lyr, and shaded boxes indicate the regions of enhanced $f_2$ amplitude. There seems to be a preference for phases close to Blazhko minima, which are also the phases where the minima of the fundamental frequency $f_0$ occur, but there is no strict rule that can predict a high $f_2$ amplitude. This irregular amplitude variability can explain the numerous peaks around $f_2$ and its combinations which can be seen in the echelle diagram (Fig. 7) and which are discussed in Section 4.1.5.

We also check the temporal variations of the frequency values of all the additional frequencies and find, in addition to the variation of $f_0$ which is plotted in Fig. 11(a), slight irregular variations of $f_1$ and $f_2$, which lead to an exact parametric resonance during some time intervals in the observed data. This might result in the momentary and transient excitation of $f_2$ which is seen in Fig. 11. We note that from the theoretical point of view, a resonance is necessary to excite the second overtone in this parameter range, because otherwise this overtone would not become unstable.

### 4.2.2 *Variation of the Blazhko modulation parameters*

The modulation parameters are normally used to describe the properties of the Blazhko modulation of a given star. The traditional parameters are $R_k = A_+/A_-$ where $A_+$ and $A_-$ are the amplitudes of the peak on the higher frequency and the lower frequency sides of the triplet, respectively, and the phase difference $\Delta\varphi_k = \varphi_+ - \varphi_-$. The parameter $k$ denotes the harmonic order. Moreover, the asymmetry parameter $Q = (A_+ - A_-)/(A_+ + A_-)$, which was introduced by Alcock et al. (2003), is widely used, as is the power difference $\Delta A^2 = A_+^2 - A_-^2$. This parameter was recently shown by Szeidl & Jurcsik (2009) to be the physically most meaningful one, as it is directly correlated to the phase difference between the amplitude and the phase modulation components in their model of modulated oscillation.

As the main aspect of V445 Lyr is the variability of the Blazhko cycles, we show here not only the average Fourier parameters for every order (which are listed in Table 3) but also their time-dependent behaviour in Fig. 12. To calculate the modulation parameters for every cycle, the data set was divided into bins, starting and ending around Blazhko minimum. The length of the bins was about 60 d, with the exception of the last bin which was only 50 d. Some overlap was allowed to guarantee frequency resolution of the Blazhko multiplet.

It was an important result for the star CoRoT 105288363 that the phasing between the two types of modulation was found to change (see section 5.3 of Guggenberger et al. 2011). Such a phase change is also indicated by the variation of $\Delta A^2$ of V445 Lyr (bottom panel of Fig. 12).

### 4.2.3 *Fourier parameters*

As the so-called Fourier parameters $R_{k1}$ (amplitude ratio) and $\varphi_{k1}$ (epoch-independent phase difference) are considered useful tools to

**Table 3.** Overall modulation parameters of V445 Lyr found from the fit to the complete data set for the first six harmonic orders.

| $k$ | $R_k$ | $\Delta\varphi_k$ | $Q_k$ | $A_k^2$ |
|---|---|---|---|---|
| 1 | 2.112 | −0.87 | 0.357 | 0.005 779 |
| 2 | 3.179 | 0.27 | 0.521 | 0.001 900 |
| 3 | 3.991 | −0.24 | 0.599 | 0.000 445 |
| 4 | 3.806 | −0.08 | 0.584 | 0.000 114 |
| 5 | 5.382 | −0.30 | 0.687 | 0.000 037 |
| 6 | 4.715 | −0.39 | 0.650 | 0.000 011 |

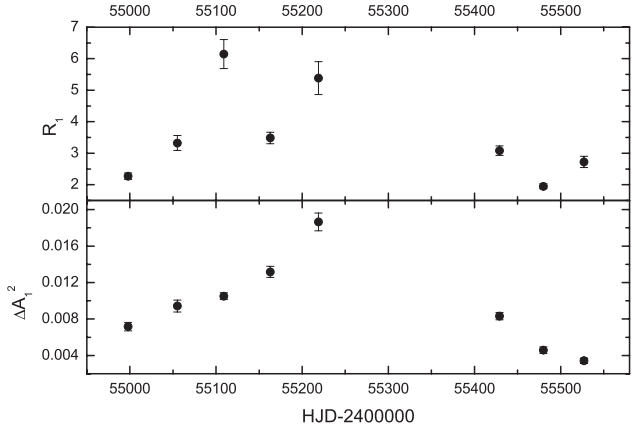


**Figure 12.** Modulation parameters of V445 Lyr versus time. The top panel shows the variation of $R_1$, which is defined as the amplitude ratio between the right and the left modulation side peak, and the bottom panel displays the variation of the power difference $\Delta A_1^2$. The variation of $\Delta A_1^2$ points towards a shift in the phasing between the two types of modulation.

study and compare the properties of RR Lyrae stars, we calculated their time variability for V445 Lyr. In contrast to the modulation parameters discussed in the previous section, they describe the pulsation rather than the modulation properties. The Fourier parameters are defined as $R_{k1} = A_k/A_1$ and $\varphi_{k1} = \varphi_k - k\varphi_1$. The data were subdivided into 239 bins of 2 d duration, therefore containing about four pulsation periods. On such short time-scales, the Blazhko effect is expected to play only a minor role. The effect of period doubling, however, causes a large error in some bins which are more affected by this effect than others. A fit including the fundamental pulsation and 10 harmonics is calculated for each bin, and the results are displayed in Fig. 13 (amplitude ratios are shown in the left-hand panels and phase differences in the right-hand panels). The average values of the parameters (derived from the complete data set) are given in Table 4.

Some interesting details are immediately obvious: while the amplitude $A_1$ of 0.18 mag is quite small compared to other RR Lyrae stars, but still in the normal range, the amplitude ratios $R_{k1}$ are significantly smaller than those of the non-modulated stars (for comparison, see fig. 6 in Nemec et al. 2011). The sharp upward spikes are an intriguing feature in the $R_{21}$ variation, which occur only during some of the observed Blazhko minima. When looking at the phases one notes that, while $\varphi_1$ has a smooth periodic variation, the phases $\varphi_2$, $\varphi_3$ and $\varphi_4$ show a more or less continuous progression (with exceptions in some cycles), leading to apparent phase jumps in the $\varphi_{k1}$ parameters.

The stability of the results was tested by also using other binnings, and the size of the bins was found to play only a minor role.

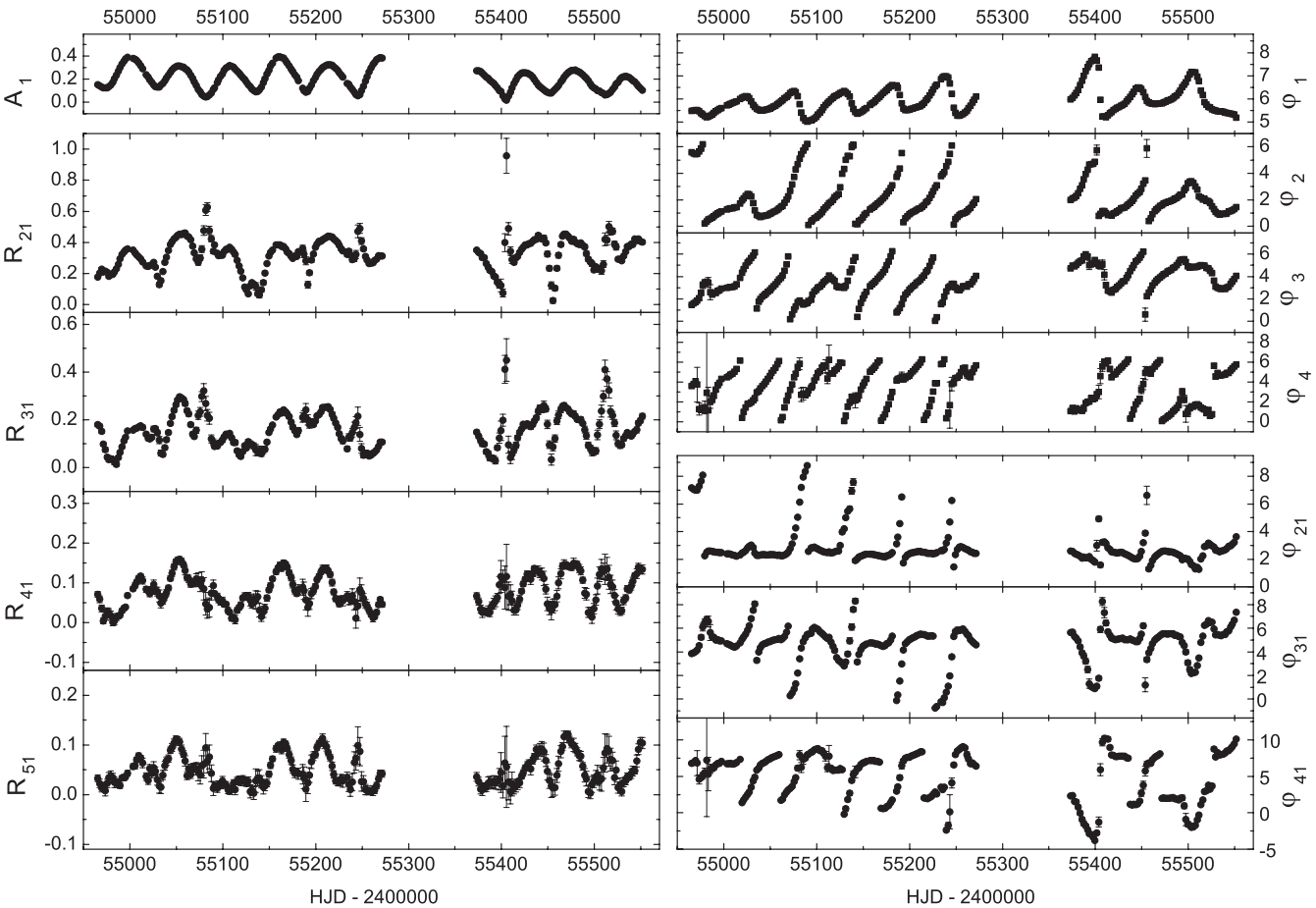


**Figure 13.** Variation of the Fourier parameters during the observed time span, calculated for subsets of 2 d duration each. Left-hand panels: at the top, the amplitude $A_1$ is displayed to indicate where Blazhko maxima and minima are located, while lower panels show the amplitude ratios $R_{21}$, $R_{31}$, $R_{41}$ and $R_{51}$. Right-hand panels: at the top, the phases $\varphi_1$, $\varphi_2$, $\varphi_3$ and $\varphi_4$ are plotted, while the lower panels show the phase differences $\varphi_{21}$, $\varphi_{31}$ and $\varphi_{41}$ in the sine frame. Where error bars are not visible, they are smaller than the symbols.

**Table 4.** Average Fourier parameters of V445 Lyr.

| Parameter | Value | Parameter | Value |
|---|---|---|---|
| $A_1$ | 0.184 | $\varphi_1$ | 5.84 |
| $R_{21}$ | 0.268 | $\varphi_{21}$ | 2.34 |
| $R_{31}$ | 0.096 | $\varphi_{31}$ | 4.95 |
| $R_{41}$ | 0.033 | $\varphi_{41}$ | 1.08 |
| $R_{51}$ | 0.013 | $\varphi_{51}$ | 3.69 |

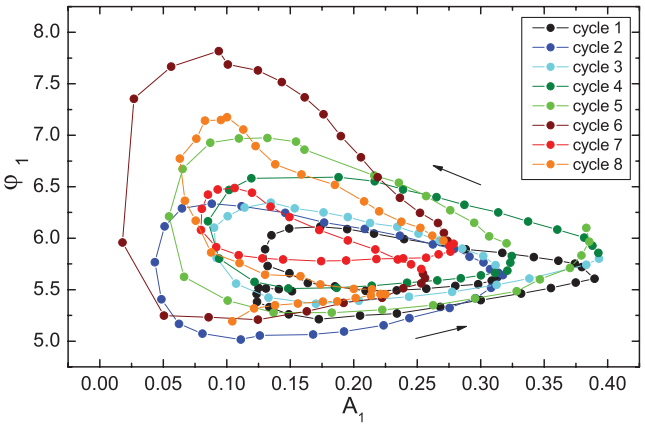


**Figure 14.** $\varphi_1$ versus $A_1$ diagram of V445 Lyr. In this plot it can be seen how various observed cycles differ from each other. Both the phase modulation component and the amplitude modulation component change over the observed time span. Moreover, their relative phasing changes from cycle to cycle.

### *4.2.4 Loop diagrams*

A good indicator for the relative contributions of phase modulation and amplitude modulation, and for the phasing between those two types of modulation, is the $A_1$ versus $\varphi_1$ diagram. The resulting loops for V445 Lyr are plotted in Fig. 14. The direction of motion is indicated with arrows. Cycles are defined for this purpose as from one maximum of $A_1$ to the next, except for the beginning and the end of the data set where additional points are added to the adjacent cycles. Cycles 1 to 5 correspond to data obtained before the gap in the observations, and cycles 6 to 8 correspond to data after the gap. Even though the contents of Fig. 14 are partly redundant with the upper panels of Fig. 13, the representation as a loop diagram allows us to better compare the observed Blazhko cycles. All observed Blazhko cycles have a different appearance in this diagram, and the contributions of amplitude and phase modulation change without notable correlation between each other.

## 4.3 O − C diagrams and long-term period change

In addition to the Fourier analysis which reveals the average Blazhko period, and the time-dependent analysis which shows the fundamental mode as a function of time, we also constructed an O − C diagram, as it can reveal additional details, especially when it comes to long-term period changes. The O − C diagram obtained from all maxima in the *Kepler* V445 Lyr light curve is shown in the top panel of Fig. 15. An intriguing feature is the non-sinusoidal variation of the O − C values with a few points at very low O − C values in some of the cycles. A closer inspection of the phase diagrams at the affected times reveals that these drops in O − C are happening at the epochs with the very unusual distorted light-curve shape showing double maxima (the double maxima are illustrated in Figs 1b and d). The determination of the time of the light maximum becomes ambiguous here, depending on the maximum that is chosen. The original maximum seems to move 'to the left' (causing negative O − C values) while a bump on the descending branch gets stronger and takes the role of the maximum for the next Blazhko cycle. This also explains the rather abrupt transition from very low to high O − C values.

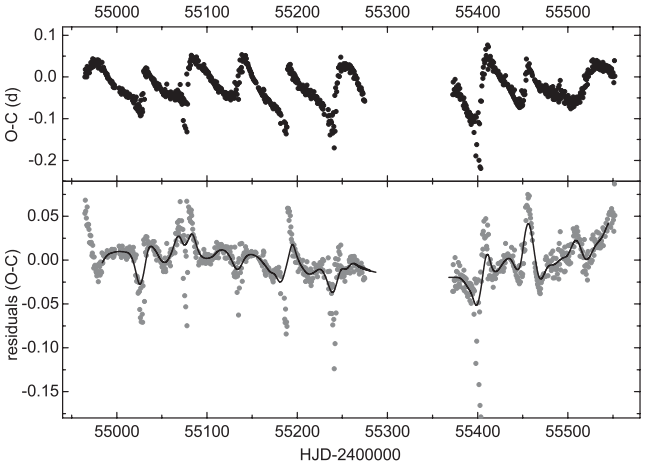


**Figure 15.** O − C diagram of the complete data set of V445 Lyr (top panel), and residuals after subtracting a fit with the Blazhko frequency, its harmonics and the secondary modulation frequency (bottom panel). To guide the eye, a line through the means of the residuals in bins of 10 maxima has been plotted.

We also performed a Fourier analysis on the O − C data to check whether the secondary modulation is also present in the phase variation. We clearly found the Blazhko frequency $f_B$, in this case 0.0184 $d^{-1}$, as well as the harmonics $2f_B$ and $3f_B$ in the O − C curve, which are introduced by the non-sinusoidal variation of the O − C curve. The secondary modulation, with a value of $f_S = 0.0064$ $d^{-1}$, as well as the combination peak $f_B + f_S$, was also directly detected in the Fourier spectrum. We note that slight differences in the frequency values obtained from the O − C diagram compared to those obtained from the magnitudes do not come unexpectedly, as the phase and AMs are not strictly correlated.

As the quasi-periodic Blazhko modulation is the dominant signal in the O − C curve, it is necessary to subtract a fit including the above-mentioned frequencies from the O − C curve to be able to identify long-term changes. The residuals of this fit are shown in the bottom panel of Fig. 15 and reveal quite clearly a long-term period change. It remains unclear, however, whether it is a periodic or a continuous linear period change.

## 4.4 The analytic modulation approach

Due to the limitations of the classical Fourier analysis discussed in Section 4, we applied a new method of analysis to the *Kepler* data of V445 Lyr, which was recently described by Benkő et al. (2011, hereafter B11). In this approach, the amplitude and frequency modulations are treated similarly to the theory of electronic signal transmission, reducing dramatically the necessary number of free parameters. This would be especially useful for stars like V445 Lyr where a classical Fourier analysis yields several hundreds of combination peaks.

As a first step of such an analysis we have to select the fitting formula, using table 1 in B11. The AM with the frequency of $f_B$ is

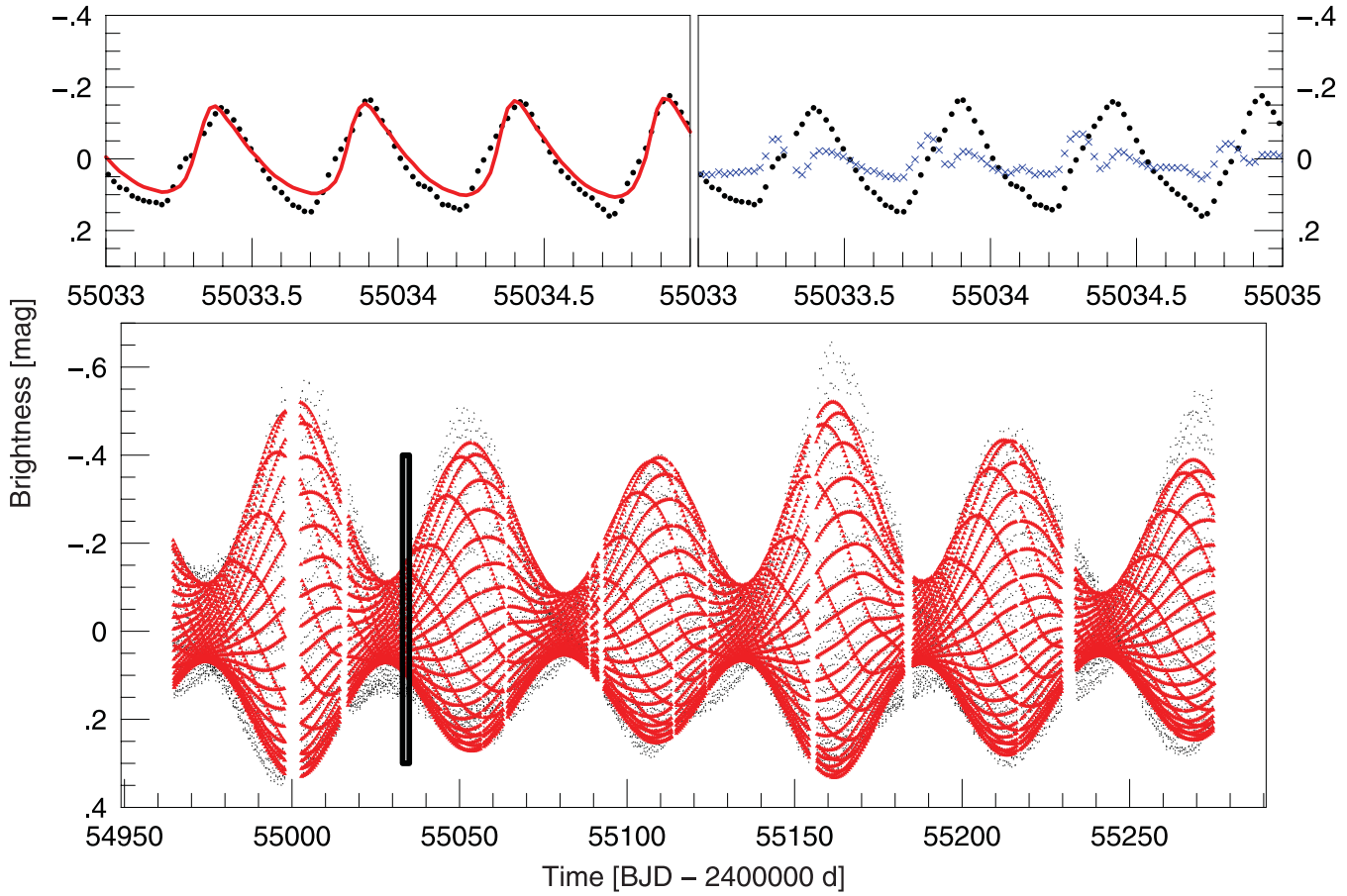


**Figure 16.** The light-curve fit of V445 Lyr during Q1–Q4 using the modulated signal approach. The bottom panel shows the global 32-parameter fit (red continuous line) with the original data (black dots). The upper panels show a local fit (left) and residual light curves (blue crosses) in the interval indicated by the rectangle in the bottom panel.

evident already from the shape of the light curve in Fig. 1. Since the envelope curve is nearly horizontally symmetric for all Blazhko cycles, the AM of $f_B$ can be approximated by a simple sinusoidal function (see formulae 20 and 21 in B11).

The high asymmetry of the multiplet peaks' amplitudes suggests a frequency modulation (FM) as well. Its non-sinusoidal nature is clear from both the frequency variation function (Fig. 11a) and the O−C diagram (Fig. 15). The combined sinusoidal AM and non-sinusoidal FM modulation of $f_B$ can be described by formula (49) in B11, where $q' = 1$.

As mentioned above V445 Lyr shows a secondary modulation $f_S$ as well, which is included in the form of an AM because of the changing amplitudes of the Blazhko cycles. As a first approximation we also assumed this modulation as sinusoidal. The linear combination of $f_B$ and $f_S$ shows interaction between the two modulations; therefore, we have to apply the formula of modulated modulation (AM cascade – equation 27 in B11).

The situation of the FM in $f_S$ is a bit controversial. The existence of an FM seems to be well established, based upon the detection of $f_S$ in the Fourier analysis of the O − C diagram; however, a combined AM with FM in $f_S$ does not improve the significance of our numerical Levenberg–Marquardt fit. This may be explained on the basis of the long cycle length of this modulation and/or its weak FM.

The used best-fitting model contains a sinusoidal AM and a non-sinusoidal FM represented by a three-term Fourier sum for the Blazhko modulation and a sinusoidal AM for the second modulation. The two modulations are assumed to be modulating each other. The free parameters are the pulsation frequency $f_0$ and its harmonics' amplitude and phase up to the ninth order ($A_1$, $A_2$, …, $A_9$, $\varphi_1$, $\varphi_2$, …, $\varphi_9$), the modulation frequency $f_B$, the amplitudes and phases of its AM ($a^A_{B1}$, $\varphi^A_{B1}$) and FM ($a^F_{Bi}$, $\varphi^F_{Bi}$, $i = 1, 2, 3$), the secondary modulation frequency $f_S$ and its AM modulation parameters ($a^A_{S1}$, $\varphi^A_{S1}$). They represent 32 parameters (with the zero-point $a_{00}$). The model light curve shows the global properties of the observed one (see Fig. 16); however, the variance of the residual (observed minus fitted) is surprisingly high (0.0025 mag).

There may be various reasons for this large variance. Some of them are method specific, others are object specific. An important limit of the method is (as mentioned by B11) that it does not describe the migration of the humps and bumps caused by the Blazhko effect, a phenomenon which is exceptionally strong in V445 Lyr. The situation is demonstrated well in the upper panels of Fig. 16. The other problem is that our method assumes regular signals. The light curve of V445 Lyr shows, however, irregular behaviour. The loop diagram in Fig. 14 illustrates the cycle-to-cycle variations of the relative strengths of the AM and FM components of the modulation. Any static (regular) models including the Fourier method face similar troubles when using them for such a time-dependent (irregular) phenomenon. Therefore, we conclude that even though applying the method leads to a success in obtaining a reasonable fit with a comparably small number of parameters, it is

nevertheless not optimal for a complicated data set like the one on V445 Lyr.

## 5 SPECTROSCOPY, COLOUR PHOTOMETRY AND FUNDAMENTAL PARAMETERS

In the framework of ground-based follow-up observations, three spectra were obtained with the HIRES spectrograph at the Keck 10-m telescope in 2011 August (Nemec, Cohen & Sesar, in preparation). Exposure times were 1200 s, and according to the ephemerides given in Section 4.1 the spectra were obtained shortly after maximum light. Due to its faintness ($Kp = 17.4$ mag), V445 Lyr is not an easy target to observe. From a preliminary analysis, heliocentric radial velocities of $-392$, $-390$ and $-388$ km s$^{-1}$, and a metallicity of [Fe/H] $= -2.0 \pm 0.3$ dex on the Carretta et al. (2009) scale, corresponding to $Z = 0.0003$, were obtained.

Based on the metallicity value derived from spectroscopy and with the frequency value of the second overtone mode, we were able to constrain the mass and luminosity of V445 Lyr with the help of a theoretical Petersen diagram which is shown in Fig. 17. Linear pulsation models (Smolec & Moskalik 2008) were calculated for a set of masses (0.55, 0.65 and 0.75 $M_\odot$, which are plotted as solid, dashed and dotted lines, respectively) and different luminosities (40, 50, 60 and 70 $L_\odot$, plotted as circles, pluses, squares and triangles, respectively). The metallicity values necessary to theoretically fit the observed frequencies agree very well with the measured metallicity, and the luminosity and mass of V445 Lyr found from Fig. 17 are 40–50 $L_\odot$ and 0.55–0.65 $M_\odot$, respectively.

As the model period ratios depend on the opacity tables and the abundance mixture used in the computations, we tested the stability of our results. The effects of different opacities and mixtures (Grevesse & Noels 1993; Asplund et al. 2009), however, were checked and found to play only a minor role. In Fig. 17, the models based on OPAL opacities and the mixture of Asplund et al. (2004) are shown. V445 Lyr is plotted as a black square in the diagram, while the other RRab stars for which the presence of the second overtone has been reported are shown as open squares. From the wide spread which the stars show in Fig. 17 it is obvious that very different parameters are needed to model different stars that show the second overtone. Larger masses are necessary to fit the period ratios of the stars with longer periods, while higher metallicities are needed to obtain a model for the shorter periods. Models for V350 Lyr and V354 Lyr have already been shown by Benkő et al. (2010) in their fig. 6 and by Nemec et al. (2011) in their fig. A2. It is already noted in Section 4.1.5 that the stars in which the second overtone is excited form a very diverse sample, therefore it is not surprising that they also cover a wide range in mass and metallicity.

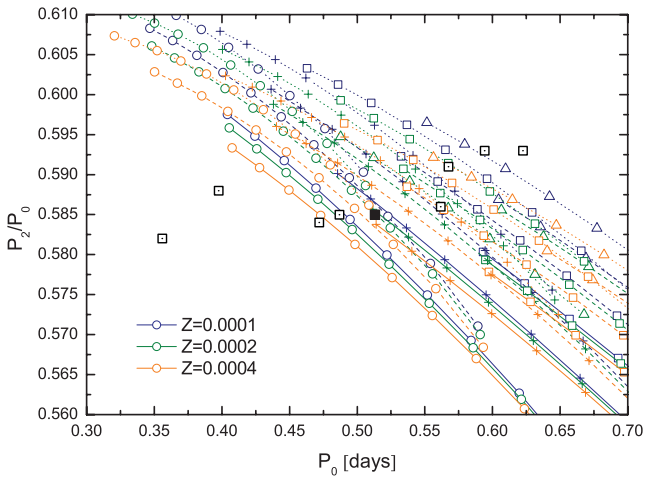


**Figure 17.** Petersen diagram for V445 Lyr (shown as black square) for the second overtone, based on models computed with the Warsaw code (Smolec & Moskalik 2008). Other RRab Lyr stars with possible second overtones (as discussed in Section 4.1.5) are plotted as open squares.

### 5.1 Ground-based colour photometry

To complement the *Kepler* data with colour information on our target, V445 Lyr was observed from the ground in *BVRI* (of which the *RI* bands are in Cousins system) using telescopes at the Lulin Observatory, including the Lulin One-metre Telescope (LOT), Lulin 0.4 m SLT and the Tenagra II Observatory (TNG, with a 0.8-m telescope). The imaging data were reduced with IRAF in a standard manner, including bias and dark subtraction, and flat-fielding. Photometry was obtained from the images using SExtractor (Bertin & Arnouts 1996), and calibrated to the standard magnitudes using standard star observation from Landolt (2009). Further details about the telescopes, the CCDs and the reduction of the imaging data can be found in Szabó et al. (2011) and Ngeow (2012), who used the same instrumentation for monitoring the Cepheid V1154 Cyg located within the *Kepler* field of view (Szabó et al. 2011).

The observations were performed between 2011 March 29 and July 24 (i.e. during the course of two Blazhko cycles) and they comprised about 70 measurements per filter with typical uncertainties of about 0.06 mag. As the data cover the pulsation cycle well, they allow the determination of an average brightness in each colour. The following average magnitudes in the standard system were obtained for V445 Lyr on the basis of the magnitudes of the single measurements: $B = 17.80$ mag, $V = 17.38$ mag, $R = 17.09$ mag and $I = 16.81$ mag.

## 6 COMPARISON WITH COROT 105288363

With the tools developed for the analysis of V445 Lyr, we revisited CoRoT 105288363 to apply the same techniques in a consistent way. Unlike in previous studies, the frequencies were kept as free parameters during the pre-whitening and fitting procedure, in spite of the increase of computing time. This has the advantage that the Blazhko period can be determined not only from one measured distance between two peaks, but also from a large number of independently detected peaks. The standard deviation of that set of measured values also gives a good error estimate. The Blazhko period found by this method is $34.6 \pm 1.1$ d and our solution agrees within the error of the previous published value of 35.6 d (Guggenberger et al. 2011).

When the echelle diagram diagnostic was applied to CoRoT 105288363, some previously undiscovered features could be unveiled. The first and most important finding is a well-resolved secondary modulation which is very similar to the one in V445 Lyr, in the sense that it has a ratio of $f_B/f_S = 2.5 \pm 0.27$ with the primary modulation, which is close to the value of $f_B/f_S = 2.7 \pm 0.12$ in V445 Lyr. Moreover, its combination peaks appear in similar positions: they are clearly found in the higher frequency side of the harmonics, and also preferentially on the higher frequency side of the classical Blazhko multiplets. The echelle diagram for CoRoT 105288363 is shown in Fig. 18. One has to note that, unlike in V445 Lyr, no systematic deviation of the harmonics from their expected positions (see Section 4.1.2) is found in CoRoT 105288363. Therefore, no tilt of the orders in the echelle diagram can be seen.

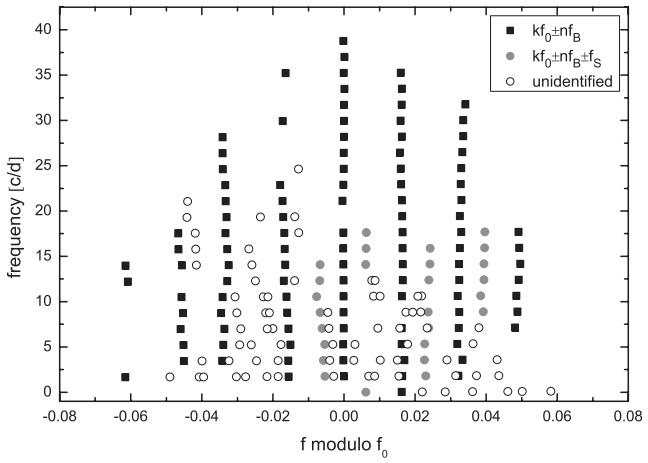


**Figure 18.** Same as Fig. 4 but for CoRoT 105288363. Note that the multiplet structure is more symmetrical than in V445 Lyr, in the sense that approximately the same number of multiplet components appear on both sides of the fundamental mode. The peaks belonging to the secondary modulation are in similar positions as in V445 Lyr. Again, several additional peaks occur which cannot be identified as combination peaks of either one of the modulations. This is most likely due to either the irregular or the yet unresolved changes of the Blazhko effect. Unlike in V445 Lyr, no combinations including a $2f_S$ term could be found.

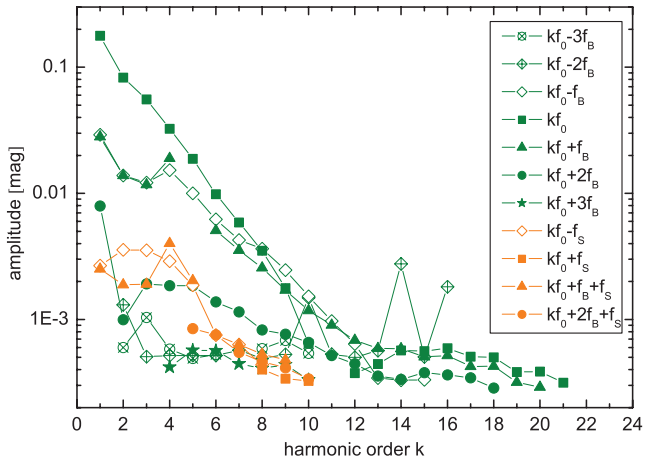


**Figure 19.** Same as Fig. 5 but for CoRoT 105288363. Here, in contrast to V445 Lyr, the components belonging to the secondary modulation never reach amplitudes higher than that of the classical multiplet, which might be connected to the fact that the changes in the Blazhko effect of CoRoT 10528836 are not so dramatic as they are in V445 Lyr. Their amplitude decrease is almost as rapid as for the classical components.

There are, however, some irregularities in the pattern with some peaks showing deviations from the exact position, though not in a systematic manner. The decrease of amplitudes of the secondary modulation components with increasing harmonic order is shown in Fig. 19. These figures should be compared to the corresponding ones for V445 Lyr (Figs 4 and 5, respectively).

The data of CoRoT 105288363 were then inspected carefully for signal outside the vicinity of the Blazhko multiplets to find evidence for overtones and other possible additional modes. The pre-whitening of not only the classical Blazhko multiplet but also the secondary modulation and the additional peaks (which also leads to the disappearance of all aliases) significantly reduced the noise level of the residuals in the frequency region of interest. The

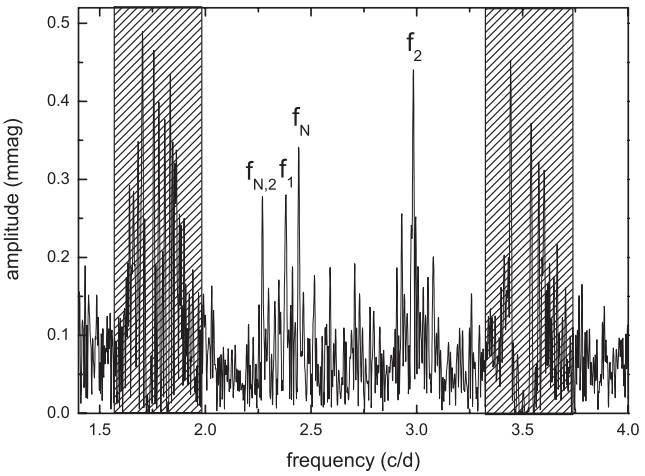


**Figure 20.** Fourier spectrum of CoRoT 105288363 after subtraction of 135 frequencies around the fundamental mode and its harmonics. A zoom into the region between $f_0$ and $2f_0$ is shown, clearly revealing the four additional peaks discussed in the text. The former positions of the multiplets around $f_0$ and $2f_0$ are marked with shaded boxes.

second overtone that was reported by Guggenberger et al. (2011) was also found in the new analysis (see Fig. 20, where it is labelled $f_2$). Due to the reduced noise, combinations of $f_2$ with $kf_0$ up to $k = 5$ could also be detected, clearly indicating that the frequency is not due to noise and is not caused by a background star. Moreover, three additional frequencies could be found (see also Fig. 20). A peak at 2.3793 $d^{-1}$ with an amplitude of 0.3 mmag is found to be most likely the first overtone due to its ratio of $f_0/f_1 = 0.741$ with the fundamental mode. Moreover, a resonance with $f_0$ and $f_2$ is possible in this case, because $2f_1 - f_2 - f_0$ is only 0.01. Another peak appears at $f_N = 2.4422$ $d^{-1}$ with an amplitude of 0.35 mmag. It cannot be attributed to any overtone. This and the fact that it appears between the positions of the first and the second overtones makes it quite similar to the observations in V445 Lyr (see Section 4.1.5). Furthermore, its amplitude is slightly higher than that of the suspected first overtone, as is the case for V445 Lyr. The third frequency found in this range is at $f_{N,2} = 2.2699$ $d^{-1}$ and has an amplitude of 0.3 mmag. It cannot be identified as a radial overtone, and it has no counterpart in V445 Lyr.

Table 5 compares the main characteristics of the two stars, including the ratios of the Blazhko modulation, while Table 6 compares the additional (overtone) modes.

**Table 5.** Comparison of the main characteristics of the two stars. The fundamental mode frequencies, the Blazhko periods and the periods of the secondary modulation are very different. Interestingly, however, the ratios between the primary and the secondary modulations are very similar.

| | CoRoT 105288363 | V445 Lyr |
|---|---|---|
| $f_0$ ($d^{-1}$) | 1.762 31 | 1.949 03 |
| $P_0$ (d) | 0.5674 | 0.5131 |
| $P_B$ (d) | 34.6 | 53.1 |
| $f_B$ ($d^{-1}$) | 0.0289 | 0.0188 |
| $f_S$ ($d^{-1}$) | 0.0115 | 0.0069 |
| $P_S$ (d) | $86.5 \pm 9$ | $143.3 \pm 5.8$ |
| $P_B/P_S$ | $2.5 \pm 0.27$ | $2.7 \pm 0.12$ |
| $P_B/P_0$ | 60.9 | 103.5 |

**Table 6.** Comparison of the overtone modes and the additional frequency of the two stars.

| | CoRoT 105288363 | V445 Lyr |
|---|---|---|
| $f_2$ (d$^{-1}$) | 2.9856 | 3.3307 |
| $A(f_2)$ (mmag) | 0.5 | 1.4 |
| $f_0/f_2$ | 0.590 | 0.585 |
| $f_1$ (d$^{-1}$) | 2.3793 | 2.6676 |
| $A(f_1)$ (mmag) | 0.3 | 2.7 |
| $f_0/f_1$ | 0.741 | 0.731 |
| $f_N$ (d$^{-1}$) | 2.442 | 2.7719 |
| $A(f_N)$ (mmag) | 0.4 | 3.6 |
| $f_0/f_N$ | 0.722 | 0.703 |

In CoRoT 105288363, there is no sign of period doubling, and no frequencies could be detected at or near the positions of the characteristic HIFs ($3f_0/2$, $5f_0/2$, etc.).

## 7 SUMMARY AND CONCLUSIONS

### 7.1 An unusual star with unusual phenomena

V445 Lyr is an RRab star with such a strong Blazhko modulation that at Blazhko minimum the peak-to-peak amplitude decreases down to 0.07 mag compared to approximately 1 mag during Blazhko maximum (a difference by a factor of 14), leading to the rather low overall amplitude $A_1$ of 0.18 mag.

The light curve around Blazhko minimum shows a strong distortion with a secondary maximum, making it impossible to even identify V445 Lyr as an RRab pulsator when observed only during Blazhko minimum.

In V445 Lyr the full variety of all the recently discovered new features in RR Lyrae stars – period doubling, strong irregular changes in the Blazhko effect, a secondary modulation, radial overtone pulsation and a non-radial mode – are combined in one single star. Therefore, it serves as an example of how ultraprecise and uninterrupted space photometry can change our view on seemingly well-known types of stars. The Fourier phases show an unusual behaviour which has not been detected before in an RR Lyrae star. Moreover, the distinct spikes in the temporal variation of the Fourier amplitude ratios are a previously unknown feature which is most likely caused by the pronounced double maximum at those phases.

### 7.2 Secondary modulation, irregular behaviour and long-term period change

In V445 Lyr, we find the most extreme variations of the Blazhko modulation known so far. This is partly, but not fully, explained by the secondary modulation of 143 d which we find in the *Kepler* data. Irregular/chaotic changes of the Blazhko modulation and/or even longer modulation periods also seem to be present, leading to a dense spectrum of peaks around the harmonics of the fundamental mode, in which with classical methods up to 771 frequencies would be found.

The amplitudes of the peaks connected to the secondary modulation were found to decrease less steeply with harmonic order than the components of the classical Blazhko multiplets. This interesting feature still awaits a physical explanation.

A long-term period change is also present, but it could not yet unambiguously be determined whether it is a periodic or a linear change (or neither). Future *Kepler* observations in the upcoming quarters will certainly reveal more about this long-term change.

### 7.3 Additional frequencies

We find at least four additional frequencies not connected to the fundamental mode, its harmonics and the Blazhko peaks. One of these peaks was interpreted as the second radial overtone, the second one could possibly be the first radial overtone, the third one was found to be due to period doubling and the fourth one was attributed to a non-radial frequency.

The second overtone is not always present during the observations. A strict dependence of the $f_2$ amplitude on the Blazhko phase could not be found. Instead, it seems to vary rather irregularly.

Amplitudes and frequencies of all additional peaks change notably during the time span of the data. It is possible that fluctuations in the frequency values of $f_1$ lead to transient resonances which temporarily excite the second overtone.

The additional peaks form numerous combinations with $f_0$ and the Blazhko multiplets (including quintuplet peaks) and also with the peaks belonging to the secondary modulation, indicating that they are all intrinsic to the target. Altogether, 80 peaks were found above the significance level at or near the combinations of those four frequencies with the other intrinsic frequencies of the target.

### 7.4 Spectroscopy, Petersen diagrams and an alternative method of light-curve analysis

Spectroscopy with the Keck telescope revealed a metallicity of [Fe/H] $= -2.0 \pm 0.3$, and Petersen diagrams based on linear pulsation models point towards a mass of 0.55–0.65 $M_\odot$ and a luminosity of 40–50 $L_\odot$.

We also applied the new analytic modulation technique to the light curve, and found that the best model contains a sinusoidal AM, a non-sinusoidal FM and a sinusoidal AM for the secondary modulation. Due to the migration of a strong bump feature and due to the irregular/stochastic changes, however, the method faces troubles similar to that of Fourier analysis.

### 7.5 Comparison with another peculiar star

A revisit of the data on CoRoT 105288363 revealed a secondary modulation period with a similar period ratio (2.5) with the primary modulation period as V445 Lyr (2.7).

The new analysis of the CoRoT 105288363 data also points towards the excitation of more additional modes than the previously published second overtone. A non-radial mode as well as the first overtone might also be excited.

V445 Lyr also shows a change in the phasing of the two types of modulation (amplitude and phase modulation), similar to what was observed in CoRoT 105288363.

## ACKNOWLEDGMENTS

Funding for this discovery mission is provided by NASA's Science Mission Directorate. EG acknowledges support from the Austrian Science Fund (FWF), project number P19962-N16. KK is presently a Marie Curie Fellow (IOF-255267). The research leading to these results has received funding from the European Commission's Seventh Framework Programme (FP7/2007-2013) under grant agreement no. 269194 (IRSES/ASK). RSz and JMB are supported by the Lendület programme of the Hungarian Academy of Sciences

and the Hungarian OTKA grants K83790 and MB08C 81013. RSz was supported by the János Bolyai Research Scholarship of the Hungarian Academy of Sciences. C-CN thanks the funding from the National Science Council (of Taiwan) under the contract NSC 98-2112-M-008-013-MY3. We acknowledge the assistance of the queue observers, Chi-Sheng Lin and Hsiang-Yao Hsiao from the Lulin Observatory, and we thank Jhen-kuei Guo and Neelam Panwar for coordinating observations at the Tenagra II Observatory. JGC and BS are grateful to NSF grant AST-0908139 for partial support. Support for MC is provided by the Ministry for the Economy, Development, and Tourism's Programa Inicativa Científica Milenio through grant P07-021-F, awarded to The Milky Way Millennium Nucleus; by Proyecto Basal PFB-06/2007; by FONDAP Centro de Astrofísica 15010003; by Proyecto FONDECYT Regular #1110326; and by Proyecto Anillo ACT-86. The authors gratefully acknowledge the entire *Kepler* team, whose outstanding efforts have made these results possible.

## REFERENCES

Alcock C. et al., 2003, ApJ, 598, 597
Arellano Ferro A., Bramich D. M., Figuera Jaimes R., Giridhar S., Kuppuswamy K., 2012, MNRAS, 420, 1333
Asplund M., Grevesse N., Sauval A. J., Allende Prieto C., Kiselman D., 2004, A&A, 417, 751
Asplund M., Grevesse N., Sauval A. J., Scott P., 2009, ARA&A, 47, 481
Benkő J. M. et al., 2010, MNRAS, 409, 1585
Benkő J. M., Szabó R., Paparó M., 2011, MNRAS, 417, 974 (B11)
Bertin E., Arnouts S., 1996, A&AS, 117, 393
Blazhko S. N., 1907, Astron. Nachr., 175, 325
Buchler R., Kolláth Z., 2011, ApJ, 731, 24
Carretta E., Bragaglia A., Gratton R., D'Orazi V., Lucatello S., 2009, A&A, 508, 695
Catelan M., 2009, Ap&SS, 320, 261
Çelik L. et al., 2012, preprint (arXiv:1202.3607)
Chadid M. et al., 2010, A&A, 510, 39
Christiansen J. L. et al., 2011, Kepler Data Characteristics Handbook (KSCI-19040-002). NASA Ames Research Center, Moffett Field, CA
Dziembowski W., Cassisi S., 1999, Acta Astron., 49, 371
Grevesse N., Noels A., 1993, in Prantzos N., Vangioni-Flam E., Casse M., eds, Origin and Evolution of the Elements. Cambridge Univ. Press, Cambridge, p. 15
Guggenberger E., Kolenberg K., Chapellier E., Poretti E., Szabó R., Benkő J. M., Paparó M., 2011, MNRAS, 415, 1577
Haas M. et al., 2010, ApJ, 713, L115
Jenkins J. M. et al., 2010, ApJ, 713, L87
Jurcsik J. et al., 2005, A&A, 430, 1049
Jurcsik J. et al., 2008, MNRAS, 391, 164
Jurcsik J. et al., 2009, MNRAS, 400, 1006
Jurcsik J. et al., 2012, MNRAS, 423, 993
Koch D. G. et al., 2010, ApJ, 713, L79
Kolenberg K. et al., 2009, MNRAS, 396, 263
Kolenberg K. et al., 2010, ApJ, 713, 198
Kolenberg K. et al., 2011, MNRAS, 411, 878
Kolláth Z., Molnár L., Szabó R., 2011, MNRAS, 414, 1111
Kukarkin B. V., Kholopov P. N., Kukarkina N. F., Perova N. B., 1973, Inf. Bull. Var. Stars, 834, 1
Landolt A. U., 2009, AJ, 137, 4186
Lenz P., Breger M., 2005, Commun. Asteroseismol., 146, 53
Nemec J. M. et al., 2011, MNRAS, 417, 1022
Ngeow C.-C., 2012, in Qian S., Leung K.-C., Zhu L., Kwok S., eds, ASP Conf. Ser. Vol. 451, The 9th Pacific Rim Conf. on Stellar Astrophysics, Astron. Soc. Pac., San Francisco, p. 103
Popielski B. L., Dziembowski W. A., Cassisi S., 2000, Acta Astron., 50, 491
Poretti E. et al., 2010, A&A, 520, A108
Reegen P., 2007, A&A, 467, 1353
Romano G., 1972, Inf. Bull. Var. Stars, 645, 1
Shapley H., 1916, ApJ, 43, 217
Smolec R., Moskalik P., 2008, Acta Astron., 58, 193
Smolec R., Moskalik P., Kolenberg K., Bryson S., Cote M. T., Morris R. L., 2011, MNRAS, 414, 2950
Sódor A. et al., 2011, MNRAS, 411, 1585
Sódor A. et al., 2012, preprint (arXiv:1201.5474v1)
Soszynski I. et al., 2009, Acta Astron., 59, 1
Soszynski I. et al., 2011, Acta Astron., 61, 1
Stothers R., 2006, ApJ, 652, 643
Szabó R., Kolláth Z., Buchler J. R., 2004, A&A, 425, 627
Szabó R. et al., 2010, MNRAS, 409, 1244
Szabó R. et al., 2011, MNRAS, 413, 2709
Szeidl B., Jurcsik J., 2009, Commun. Asteroseismol. 160, 17
Van Cleve J., Caldwell D. A., 2009, Kepler Instrument Handbook (KSCI 19033). NASA Ames Research Center, Moffett Field, CA
Van Hoolst T, Dziembowski W. A., Kawaler S. D., 1998, MNRAS, 297, 536

## SUPPORTING INFORMATION

Additional Supporting Information may be found in the online version of this article:

**Table 1.** The scaled and detrended data set of V445 Lyr that was used for the analysis in this paper.

Please note: Wiley-Blackwell are not responsible for the content or functionality of any supporting materials supplied by the authors. Any queries (other than missing material) should be directed to the corresponding author for the article.

This paper has been typeset from a TEX/LATEX file prepared by the author.